Bioorganic Chemistry 89 (2019) 103006

Contents lists available at ScienceDirect

Bioorganic Chemistry

journal homepage: www.elsevier.com/locate/bioorg

Design, synthesis and biological activity of novel tacrine-isatin Schiff base hybrid derivatives

E. Riazimontazer[a], H. Sadeghpour[a,*], H. Nadri[b], A. Sakhteman[a,1], T. Tüylü Küçükkılınç[c], R. Miri[a,d], N. Edraki[d]

[a] Department of Medicinal Chemistry, School of Pharmacy, Shiraz University of Medical Sciences, Shiraz, Iran
[b] Department of Medicinal Chemistry, Faculty of Pharmacy and Pharmaceutical Sciences Research Center, Shahid Sadoughi University of Medical Sciences, Yazd, Iran
[c] Hacettepe University, Faculty of Pharmacy, Department of Biochemistry, Sihhiye-Ankara, Turkey
[d] Medicinal and Natural Products Chemistry Research Center, Shiraz University of Medical Sciences, Shiraz, Iran

ARTICLE INFO

Keywords:
Alzheimer's disease
Acetylcholinesterase
Butyrylcholinesterase
Cholinesterase inhibitors
Tacrine
Isatin Schiff base
Amyloid-beta aggregation
Metal chelation

ABSTRACT

A series of novel tacrine-isatin Schiff base hybrid derivatives (**7a-p**) were designed, synthesized and evaluated as multi-target candidates against Alzheimer's disease (AD). The biological assays indicated that most of these compounds displayed potent inhibitory activity toward acetylcholinesterase (AChE) and butyrylcholinesterase (BuChE) and specific selectivity for AChE over BuChE. It was also found that they act as excellent metal chelators. The compounds **7k** and **7m** were found to be good inhibitors of AChE-induced amyloid-beta (Aβ) aggregation. Most of the compounds inhibited AChE with the IC_{50} values, ranging from 0.42 nM to 79.66 nM. Amongst them, **7k**, **7m** and **7p**, all with a 6 carbon linker between tacrine and isatin Schiff base exhibited the strongest inhibitory activity against AChE with IC_{50} values of 0.42 nM, 0.62 nM and 0.95 nM, respectively. They were 92-, 62- and 41-fold more active than tacrine (IC_{50} = 38.72 nM) toward AChE. Most of the compounds also showed a potent BuChE inhibition among which **7d** with an IC_{50} value of 0.11 nM for BuChE is the most potent one (56-fold more potent than that of tacrine (IC_{50} = 6.21 nM)). In addition, most compounds exhibited the highest metal chelating property. Kinetic and molecular modeling studies revealed that **7k** is a mixed-type inhibitor, capable of binding to catalytic and peripheral site of AChE. Our findings make this hybrid scaffold an excellent candidate to modify current drugs in treating Alzheimer's disease (AD).

1. Introduction

Alzheimer's disease (AD) is a progressive and fatal degenerative disorder in the central nervous system leading to the most common form of dementia in aged population [1]. Patients suffer from AD have symptoms such as memory loss and other cognitive disabilities. The slowly developing symptoms are serious enough to interfere with daily tasks that eventually lead to mortality. At the moment, about 40 million people worldwide are affected by AD and by 2050 it will affect 150 million people [2]. Constant care and related services cost billions of dollars annually, including medical care, and human resources. Today, AD is considered as one of the most expensive diseases and the expenses is expected to increase by fivefold in the year 2050 [3,4]. Although some cases of AD were observed before the age of 65, old age is one major known risk factor for this disease [5]. Since the current AD treatments are not curable, finding better treatment strategies has become a worldwide endeavor. Most studies focused on finding remedies, to retard its onset and stop it from progression [6,7].

Autopsy studies and clinical diagnoses have confirmed major pathological hallmarks for AD in the basal forebrain, cortex and amygdale [8]. Intracellular formation of neurofibrillary tangles (NFTs) and neuropil threads (NTs) resulting from abnormal hyperphosphorylation of tau protein is of a great importance [9]. In addition, the aggregation and extracellular deposition of amyloid beta (Aβ) protein is the cause of plaque formation [10]. Recently, these small oligomers of β-amyloid and tau protein have gained considerable attention. It is associated with the hydrolysis of the amyloid precursor protein (APP) by β-secretase 1 (BACE-1) [11]. They were found to be effective in activating apoptotic cascade leading to cell death [12]. Other factor involved in AD is reduced cholinergic transmission and acetylcholine (ACh) levels which makes it a prominent strategy for developing cholinesterase inhibitors (ChEIs). The aim of cholinesterase inhibitors is to increase the levels of

* Corresponding author.
E-mail addresses: sadeghpurh@sums.ac.ir (H. Sadeghpour), asakhteman@sums.ac.ir (A. Sakhteman).
[1] Co-corresponding author.

https://doi.org/10.1016/j.bioorg.2019.103006
Received 8 December 2018; Received in revised form 10 March 2019; Accepted 19 May 2019
Available online 21 May 2019
0045-2068/

acetylcholine through inhibition of cholinesterases (ChEs) [13]. Acetylcholinesterase (AChE) is also accountable for several non-catalytic pro-aggregation activity [14]. Peripheral anionic site (PAS) amino acid residues in AChE can interact with Aβ protein to produce AChE-Aβ complex, found to be entangled in Aβ aggregates [15]. Aβ as a metalloprotein has selective high- and low-affinity metal binding sites [16]. High level of iron, copper and zinc in cerebral β-amyloid deposits can also speed up Aβ aggregation [17]. Metal chelators and ROS scavengers have potential therapeutic capacity in treating AD due to increased level of metal ions in plaques [18]. Based on distinctive structural and biochemical properties of AChE, molecules with specific interaction with catalytic active site (CAS) and peripheral anionic site (PAS) residues can be important in AChE inhibition. These agents are also helpful in preventing Aβ aggregation facilitated by AChE [19,20]. The hydrolyzing effect and therefore termination of ACh activity in case of both cholinesterase enzymes (AChE and BuChE) plays an important role in different regions of the brain. In AD, a decrease in AChE turnover by up to 85% is observed in particular parts of the brain. In contrast, Butyrylcholinesterase (BuChE) levels are amplified during the development of AD [21]. Indeed, the increase ratio of BuChE to AChE in AD brain can improve the supportive role of BuChE in hydrolyzing excess of ACh. In addition, formation of hallmarks such as amyloid rich neuritic plaques and neurofibrillary tangles were discovered by increasing levels of BuChE [22].

The first and the only class of drugs in the market, for treating AD are cholinesterase inhibitors, such as tacrine, donepezil, rivastigmine, galantamine and memantine [23–25]. Thus, as an efficient therapy, incorporation of a known AChE inhibitor, which is linked with another moiety to create bi- or multifunctional hybrid exerts beneficial properties in the treatment of AD [26]. The AChE and BuChE moieties of the hybrid structures are constructive in the interaction of molecules with PAS as well as CAS [27]. Tacrine (1,2,3,4-tetrahydroacridin-9-amine) is a reversible inhibitor of cholinesterase and the first FDA approved drug for AD. Although, its side effects such as serious hepatotoxicity has limited its usage in therapeutic application; hence, modifying this compound is still of great interest [28]. With respect to designing hybrid structures, some multi-target compounds were designed by connecting tacrine with another fragment through a proper linker in order to develop potent ChEIs with additional activities [29]. For example, tacrine-rhein hybrids [30], tacrine-coumarin hybrids [31], donepezil-tacrine hybrids [32] and tacrine-melatonin hybrids [33] are reported as multifunctional agents.

In this work, isatin (1H-indole-2,3-dione) was selected as a molecular fragment to design a novel tacrine-isatin Schiff base hybrid with multi-target characteristic. It is an endogenous low molecular weight non-peptide compound which is used for the synthesis of large variety of heterocyclic compounds and has many interesting biological activities [34,35]. It is found in mammalian tissues and body fluids and its modulator function has been the subject of several studies [36,37]. The studies suggested that isatin increased ACh levels by inhibiting AChE activity. Some derivatives such as isatin Mannich bases were considered to develop new cholinesterase and carbonic anhydrase (CA) inhibitors [38]. Isatin as an endogenous inhibitor of monoamine oxidase (MAO), especially MAO-B, may play a role in the regulation of the brain levels of acetylcholine and dopamine, which are reduced in age dependent neurodegenerative diseases such as AD and parkinson [39–41]. The neuroprotective property of isatin is also mainly related to the inhibition of monoamine oxidase. Isatin as a bioregulator has a selective effect on certain protein-protein interactions (PPI) [42,43]. It may influence interaction between amyloid-beta and its crucial intracellular targets and this opens new possibilities in pharmacological prevention of amyloid-beta toxicity [44,45]. The scavenging and antioxidant activity of isatin derivatives were also reported [46,47]. Amongst all activity profiles, the inhibition of enzymes (cholinesterase, carbonic anhydrase, MAO-B), the effect on protein aggregations, neuroprotective properties and antioxidant activity can make isatin a good candidate to design multifunctional molecules against neurodegenerative diseases.

The other approach to design tacrine-isatin Schiff base hybrids was based on structural modification of donepezil by using indole moiety as a bioisosteric substitute of the indanone moiety of donepezil which is available in isatin structure [48–50]. Some isatin bioisosteric structures have been reported as dual inhibitors of AChE and BACE-1 as well [51,52]. Structures of several previously reported compounds related to donepezil and isatin structure with their activity profiles have been shown in Scheme 1.

As the main purpose of the present study, a selection of novel tacrine-isatin Schiff base hybrid derivatives was consequently synthesized and their structures were clarified. The synthesized compounds were evaluated for their *in vitro* activity as inhibitors of AChE, BuChE, and amyloid-beta anti-aggregation activity, with metal chelation properties.

2. Result and discussion

2.1. Chemistry

The tacrine-Schiff base hybrids **7a-p** were synthesized by the following route depicted in (Scheme 2). At the beginning of this synthetic strategy, tacrine **2** was prepared according to the well-known Friedländer condensation reaction between anthranilonitrile and cyclohexanone. The reaction was promoted by a lewis acid, aluminium chloride, as a catalyst [53]. The subsequent step was done by the reaction of tacrine with dibromoalkanes in the presence of sodium hydride in a dry condition to provide the intermediates **3a** and **3b**. The optimal linker length in terms of the possibility of reaction and eligible yield was n = 5, 6. Afterwards, isatin reacted with different aniline derivatives, substituted by electron withdrawing and electron donating groups in *para*, *metha* and *ortho* positions, to produce isatin-Schiff base derivatives as another key intermediates **6a-h**. Isatin-Schiff base compounds were obtained by condensation reaction under reflux in ethanolic solution in the presence of catalytic amount of acetic acid for 5–6 h in good yields [54]. Finally, **3a** or **3b** was reacted with the mentioned isatin-Schiff base derivatives **6a-h** to form a desired compounds **7a-p** in good yields. Nucleophilic reactions in the presence of potassium carbonate at room temperature and dry DMF afforded desired target compounds **7a-p** in good yields.

2.2. Structure-Activity relationship of the compounds 7a-p

Based on the distance between CAS and PAS of the AChE, different structures of tacrine-isatin Schiff base with 5 and 6 carbon linkers were synthesized. The aim was to achieve the optimal linker length for the activity of this series of compounds. Another perspective of this study was to investigate the role of electron donating and electron withdrawing groups at different positions of isatin. For this purpose, different groups including -Me, -OMe, -NO_2, -Cl, were introduced to 2-, 3- or 4-position of isatin Schiff base moiety (phenyl ring), to afford the compounds 7b-h and 7j-p. Synthesis of the compounds 7a-p is depicted in Scheme 2.

After obtaining all the target compounds, their inhibitory activities against acetylcholinesterase (AChE, from electric eel) and butyrylcholinesterase (BuChE, from equine serum) were determined according to Ellman's method, using tacrine as a reference compound [55]. The IC_{50} values of all tested compounds and their selectivity index for eelAChE over eqBuChE are summarized in Table 1. Hence, it can be concluded that most of the tested compounds (7a-7p) are potent ChE inhibitors with IC_{50} values ranging from 0.42 nM to 79.66 nM. Compounds (7i-p) with six-carbon linker between tacrine moiety and isatin Schiff base showed inhibitory activity toward AChE better than compounds (7a-h) with five-carbon linker. Furthermore, the optimal linker length, seen in the 6-carbon compounds afforded better selectivity towards AChE (Table1). Amongst the compounds with 6 carbon linker, compounds 7k, 7m and 7p substituted with 3-chloro group

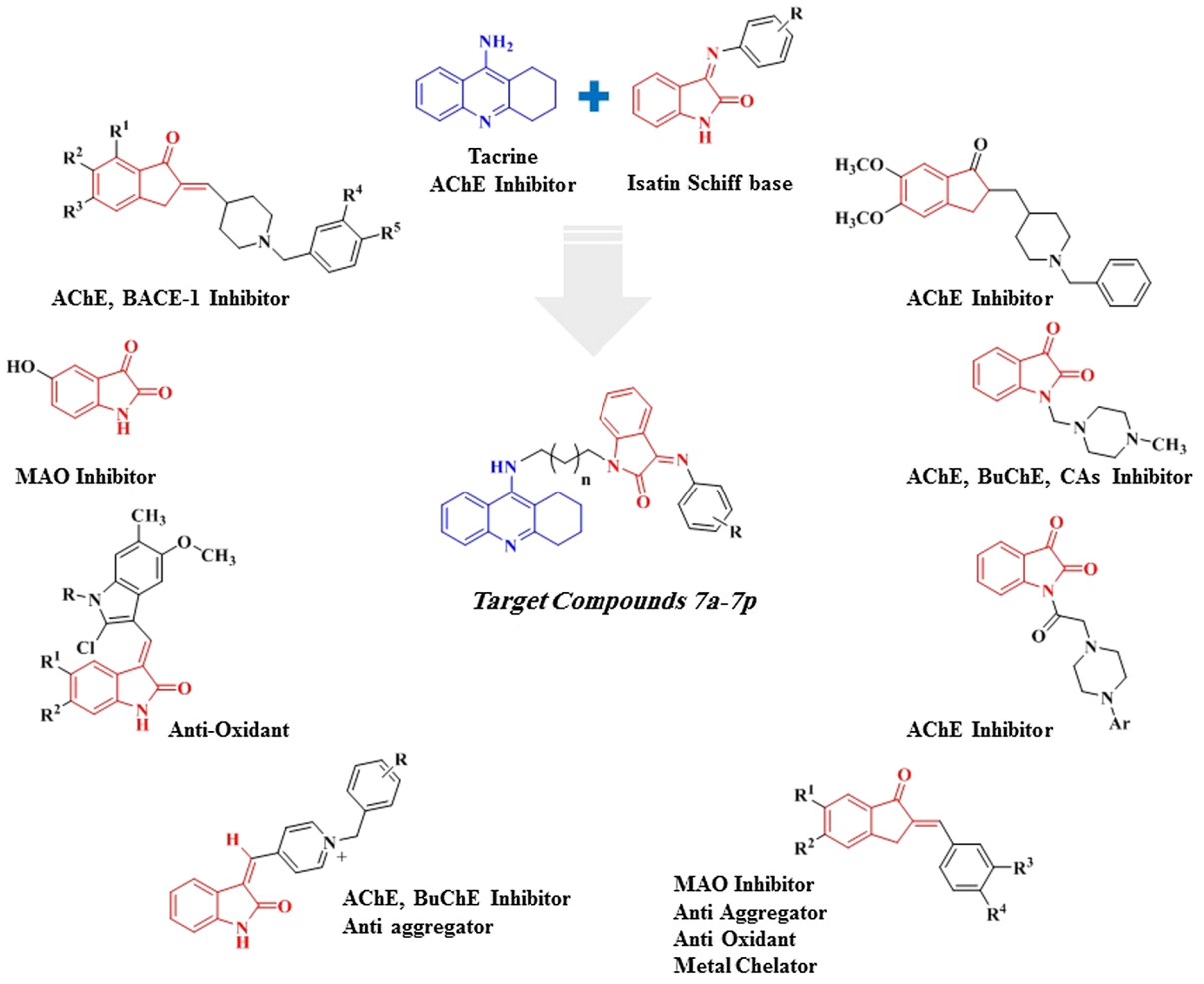

Scheme 1. Structures of some anti-Alzheimer compounds related to donepezil and isatin structures with their biological properties.

(IC_{50} = 0.42 nM), 3-nitro group (IC_{50} = 0.62 nM) and 4-methoxy group (IC_{50} = 0.95 nM) had the highest AChE inhibitory activity. The activity of these compounds is 92-, 62- and 41-fold more potent than that of tacrine (IC_{50} = 38.72 nM for AChE). In 6 carbon linker series, 7j with IC_{50} = 2.79 nM exerted the minimum inhibitory activity against AChE, which is 14-fold more potent than tacrine. Both potential ligands had chloro and nitro groups as electron-withdrawing substituent at *meta* position (7k, 7m). Moving the chloro group at 3-position of isatin Schiff base ring in compound 7k (IC_{50} = 0.42 nM) to 2 and 4-position in compound 7j (IC_{50} = 2.79 nM) and 7n (IC_{50} = 1.63 nM) resulted in a significant reduction in AChE inhibition. The results revealed that the inhibitory activity for AChE could be increased with an electron-deficient substituent at *meta* position. Amongst 5 carbon linker series for AChE, compounds 7c (IC_{50} = 15.37 nM) and 7e (IC_{50} = 7.30 nM) showed to have higher potency than others, which is 2.5- and 5-fold more potent than tacrine. In this case, the same pattern was perceived as well as the compounds with 6 carbon linker. Both 7c and 7e bearing chloro and nitro withdrawing groups in *meta* position. These results implied that n = 6 might be a suitable length for linker to bind simultaneously to PAS and CAS of AChE.

The activity of the compounds against BuChE is shown in Table 1. Compound 7d with a five carbon linker exhibited the strongest inhibition against BuChE with IC_{50} value of 0.11 nM, which was 56-fold more potent than that of tacrine (IC_{50} = 6.21 nM). However, for other compounds, a comparative trend was observed with lengthening the linker and changing the substituted groups. As a result, in compounds bearing nitro at *meta* position and methoxy at *para* position, changing linker length from 5 to 6 decreased BuChE inhibition ((7e, 7m) and (7h, 7p)). In contrast, in case of chloro analogues, an increase in BuChE inhibitory activity was observed by lengthening alkyl chain spacer from 5 to 6 carbon atoms ((7b, 7j), (7c, 7k) and (7f, 7n)). In methyl substituted compounds 7d, 7l, 7g and 7o a different pattern was figured out. 3-methyl in 5 carbon linker compound (7d) showed a higher potency than its congener with 6 carbon linker (7l). On the contrary, in compounds with methyl at position 4 (7g, 7o), lengthening the linker from 5 to 6 gave higher BuChE inhibitory activity.

On the other hand, by replacing chloro group at 3-position of isatin Schiff base moiety (compound 7k, IC_{50} = 0.42 nM) with nitro group in compound 7m (IC_{50} = 0.62 nM), the AChE inhibitory activity dropped slightly, while the BuChE inhibitory activity decreased significantly (compound 7k with IC_{50} = 0.57 nM and compound 7m with IC_{50} = 3.52 nM). It was concluded that nitro group was unfavorable for BuChE inhibition, and such an unbalanced decline in AChE and BuChE inhibition led to the high selectivity index (SI = 5.677) for 7m. The same pattern was observed for 7p with methoxy group at *para* position (IC_{50} = 0.95 nM for AChE and IC_{50} = 6.05 nM for BuChE), which resulted in the highest selectivity index (SI = 6.368). It could be inferred that 6 carbon linker with substituent at *para* position causes an increase in the selectivity index of compounds.

2.3. Kinetic study of AChE inhibition

To survey the inhibition mechanism of AChE, compound 7k as the most potent inhibitor was selected for kinetic studies by analyzing

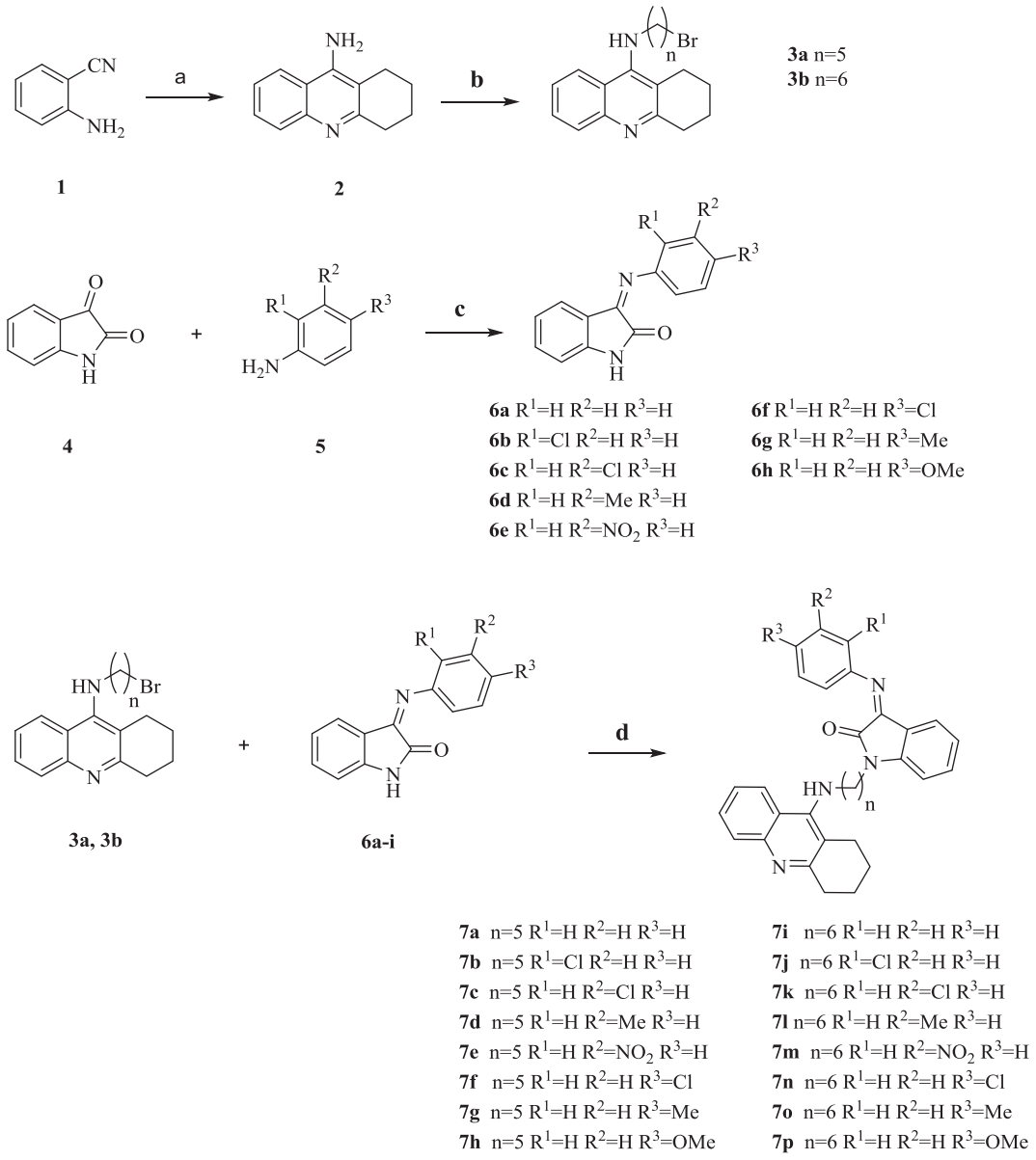

Scheme 2. Synthesis of tacrine-isatin Schiff base hybrids **7a-p**. Reagents and conditions: (a) i) cyclohexanone, toluene, $AlCl_3$, reflux, 24 h; ii) NaOH, reflux, 24 h; (b) $Br(CH_2)_nBr$ (n = 5,6), NaH, dry DMF, r.t., 5 h (c) acetic acid, ethanol, reflux (d) anhydrous K_2CO_3, dry DMF, r.t., 24 h.

Lineweaver–Burk plots. This method provides information about the mode of inhibition and binding of these inhibitors. This graphical plot represents reciprocal velocity versus reciprocal substrate ATChI (acetylthiocholine iodide) on three increasing concentrations for the different inhibitor concentrations. As shown in Fig. 1, increased slopes (from 0.03 to 0.195) and intercepts (from 0.35 to 0.85) at following increasing concentration of the inhibitor 0, 1.13, 2.22 and 4.32 nM, indicated a mixed-type inhibition. This pattern indicates that compound 7k might have affinity to peripheral anionic site (PAS) as well as catalytic anionic site (CAS) of AChE. Previous studies showed that some amino acids in PAS of AChE are responsible for interaction with Aβ peptide, which might induce the deposition of neurotoxic Aβ fibrils. As a result, inhibitors with the ability to bind to both CAS and PAS of AChE and mixed-type inhibition mechanism might be able to reduce amyloid plaque formation as well as AChE inhibitory activity. Compound 7k, with a six carbon linker length between tacrine and isatin Schiff base, can concurrently interact with the CAS and PAS of AChE that has potential inhibitory activity to AChE- induced Aβ aggregation. As a secondary plot, by applying the slope values of the Lineweaver-Burk plots versus varying concentration of 7k, the inhibition constant value, Ki, equal to 0.41 nM was found for compound 7k (Fig. 1).

2.4. Molecular docking

2.4.1. Docking study with AChE

As an attempt to find the binding pose of the most potent compounds 7k, 7m and 7p in the active site of AChE, the ligand-protein docking was carried out by means of Auto Dock Vina (1.1.2). The Protein Data Bank (PDB) contains variety of crystal structures of acetylcholinesterase complexed with different ligands. For this aim, five 3D X-ray crystal structures of AChE were retrieved from Protein Data Bank (PDB). Amongst them, 4EY7, 1E66 and 1EVE were selected based on optimal self-docking criteria of RMSD $<$ 2. The best docking validation score belonged to 1E66 (RMSD = 0.60). The obtained parameters from validation step were used for cross-docking of the synthesized compounds. After termination of cross-docking simulation, the best pose for each ligand was selected for visualization and analysis. The results of cross-docking studies in terms of binding energies together with the

Table 1
Inhibition of eelAChE and eqBuChE by compounds 7a-p.

Compound	n	R^1	R^2	R^3	IC_{50} (nM)		Selectivity index[c]
					eelAChE[a]	eqBuChE[b]	
7a	5	H	H	H	39.98 ± 0.23	2.67 ± 0.14	0.07
7b	5	Cl	H	H	35.94 ± 1.02	2.49 ± 0.44	0.07
7c	5	H	Cl	H	15.37 ± 0.58	1.34 ± 0.02	0.09
7d	5	H	Me	H	57.85 ± 3.36	0.11 ± 0.02	0.00
7e	5	H	NO_2	H	7.30 ± 0.02	3.14 ± 0.11	0.43
7f	5	H	H	Cl	16.32 ± 0.37	2.96 ± 0.31	0.18
7 g	5	H	H	Me	79.66±10.15	2.80 ± 0.67	0.03
7 h	5	H	H	OMe	35.17± 0.98	0.59 ± 0.05	0.02
7i	6	H	H	H	2.52 ± 0.26	4.19 ± 0.13	1.66
7j	6	Cl	H	H	2.79 ± 0.14	2.14 ± 0.18	0.77
7k	6	H	Cl	H	0.42 ± 0.01	0.57 ± 0.10	1.36
7l	6	H	Me	H	2.41 ± 0.08	0.46 ± 0.02	0.19
7m	6	H	NO_2	H	0.62 ± 0.06	3.52 ± 0.44	5.68
7n	6	H	H	Cl	1.63 ± 0.13	2.86 ± 0.02	1.75
7o	6	H	H	Me	2.69 ± 0.17	0.94 ± 0.09	0.35
7p	6	H	H	OMe	0.95 ± 0.21	6.05 ± 0.38	6.37
Tacrine					38.72 ± 3.16	6.21 ± 0.58	0.16

[a] The 50% inhibitory concentration (means ± SD of three experiments) of AChE from electric eel.
[b] The 50% inhibitory concentration (means ± SD of three experiments) of BuChE from equine serum.
[c] AChE selectivity index = IC_{50} (eqBuChE)/ IC_{50} (eelAChE).

residues involved in the interaction are shown in Table 2 for all three PDB codes. As it can be seen from the results of interaction for three PDB codes, all are in good agreement. The molecular docking results for representative compounds 7k, 7m and 7p showed that the ligands were well oriented towards the bottom of the active site gorge.

As shown in Fig. 2, the tacrine moiety of 7k, 7m and 7p were situated at the CAS of AChE (1E66). Tacrine ring and protonated nitrogen created π-π stacking interaction and cation-π interaction with the indole ring of Trp84 and phenyl ring of Phe330. The positively charged nitrogen of tacrine made a hydrogen bond with His440. In addition, the positively charged nitrogen of Schiff base could interact with Trp279 via a cation-π interaction and also showed π-π stacking interaction with the Schiff base ring in the PAS of AChE (1E66).

The nitrogen attached to the linker by tacrine in 7p, interacted with Trp84 by cation-π interaction in the CAS and the protonated nitrogen of isatin created cation-π interaction with Tyr334 in the PAS of AChE (1EVE). In contrast, the tacrine ring in 7k and 7m adopted an inverse orientation through π-π stacking against the indole ring of Trp 279 in PAS, while Schiff base ring formed π-π interaction with Trp84 in the CAS. Also, Tyr334 and Phe330 adopted cation-π interactions through protonated nitrogen of isatin and nitrogen of Schiff base in the CAS of AChE (1EVE). Thy121 and Tyr334 are the two residues responsible for interactions with the mid-gorge of AChE (1EVE) (Fig. 2).

The tacrine ring in 7k, 7m and 7p adopted π-π stacking orientation by Trp86 and cation-π interaction by Trp86 and Tyr337. Nitrogen attached to the linker by tacrine, at the CAS was responsible for the two interactions. In 7m, nitrogen of Schiff base interacted with Trp286 ring through cation-π interaction with the PAS of AChE (4EY7). Formation of hydrogen bonds was observed between hydroxyl groups of Tyr124 and Phe295 and carbonyl group in isatin at the PAS of AChE (4EY7). This led to more stabilized interaction. Isatin could bind to the mid-gorge site of AChE (4EY7) through a cation-π interaction between its protonated nitrogen atom and Tyr341.

The above kinetic study implied that 7k, 7m and 7p were a dual site binding inhibitor for AChE. In fact, the present molecular docking results confirmed that these compounds bind to CAS, PAS and mid-gorge site of AChE simultaneously. These results were consistent with our molecular design for AChE inhibition.

2.4.2. Docking study with BuChE

Due to the significant potency of target compounds on BuChE, ligand–protein docking was also conducted to predict the binding poses of the representative compounds 7d, 7h and 7l in the active site of BuChE. The 3D coordinate of the human BuChE (PDB ID: 4XII) was retrieved and prepared as described for AChE. Docking of 7d, 7h and 7l was performed after a self-docking validation procedure (RMSD = 1.59 A°). As depicted in Fig. 3, compounds 7d, 7h and 7l were well fitted in the active site cavity of BuChE. The fused tacrine ring was oriented to hydrophobic pocket composed of Trp82 with cation-π interaction and$\pi - \pi$ stacking interaction. In 7d, the oxygen atom of the isatin ring contributed to hydrogen-binding with Thr120. In 7h, theπ-cation interaction and $\pi - \pi$ stacking interaction formed by Tyr332 with nitrogen and phenyl ring of Schiff base. In 7l, π-cation interaction with Tyr332 and protonated nitrogen of isatin ring were seen. The results showed that all the three compounds could bind to CAS and PAS of the BuChE (Table 3).

2.5. Ferrous (Fe^{2+}) ions chelating activity

Fe^{2+} as a transition metal ion has the ability to form free radicals by

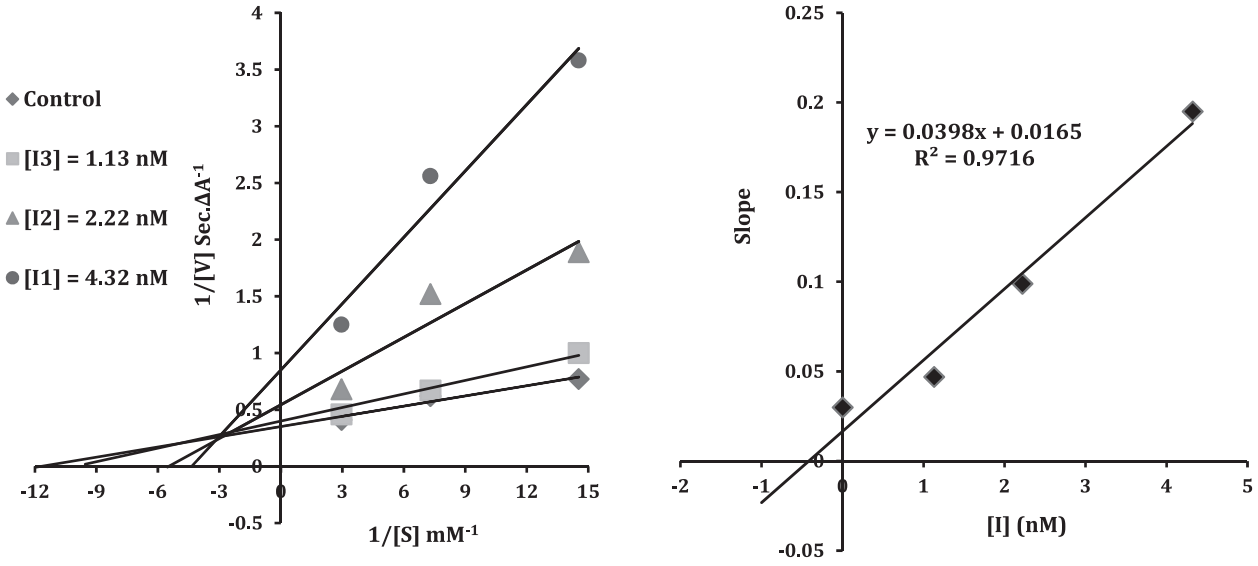

Fig. 1. Kinetic of AChE inhibition by compound 7k: (Left) Lineweaver-Burk plot, (Right) Lineweaver-Burk secondary plot.

Table 2
RMSD values and binding energies of compounds 7k, 7m and 7p with the residues involved in the intractions.

PDB Code	RMSD of self-docking	Binding Energy (Kcal.mol^{-1})				7k		7m		7p		Tacrine
		7k	7m	7p	Tacrine	CAS	PAS	CAS	PAS	CAS	PAS	CAS
1E66	0.60	−13.4	−13.7	−12.8	−10.0	Trp84 Phe330 His440	Trp279	Trp84 Phe330 His440	Trp279	Trp84 Phe330 His440	Trp279	Phe330 Trp84 His440
1EVE	0.86	−12.6	−12.3	−12.0	−8.4	Trp84 Tyr334 Phe330	Trp279	Tyr334 Phe330	Trp279	Trp84 Tyr121	Tyr334	Phe331 Phe330 Asp72
4EY7	0.98	−13.2	−13.8	−13.0	−8.8	Trp86 Tyr337	Tyr341 Phe295	Trp86 Tyr337	Tyr341 Trp286 Tyr124	Trp86 Tyr337	Tyr341 Phe295	Phe338 Tyr337 His447 Tyr124

gaining or losing electrons. Therefore, reactive oxygen species formation can be prevented by the chelation of metal ions with chelating agents. In the present study, chelation power assay was done on the new tacrine isatin Schiff base derivatives by assessing their ability to compete with ferrozine for ferrous ion [56]. In the presence of chelating agents, the formation of ferrozine-Fe^{2+} complex with a magenta color is not completed, leading to reduced absorbance. Our data is shown in Table 4. Most of the compounds have significant chelation power (33–81%) in comparison with tacrine (83%) and EDTA (84%) as a standard iron chelator (Fig. 4). It was observed that 7k and 7p exhibited

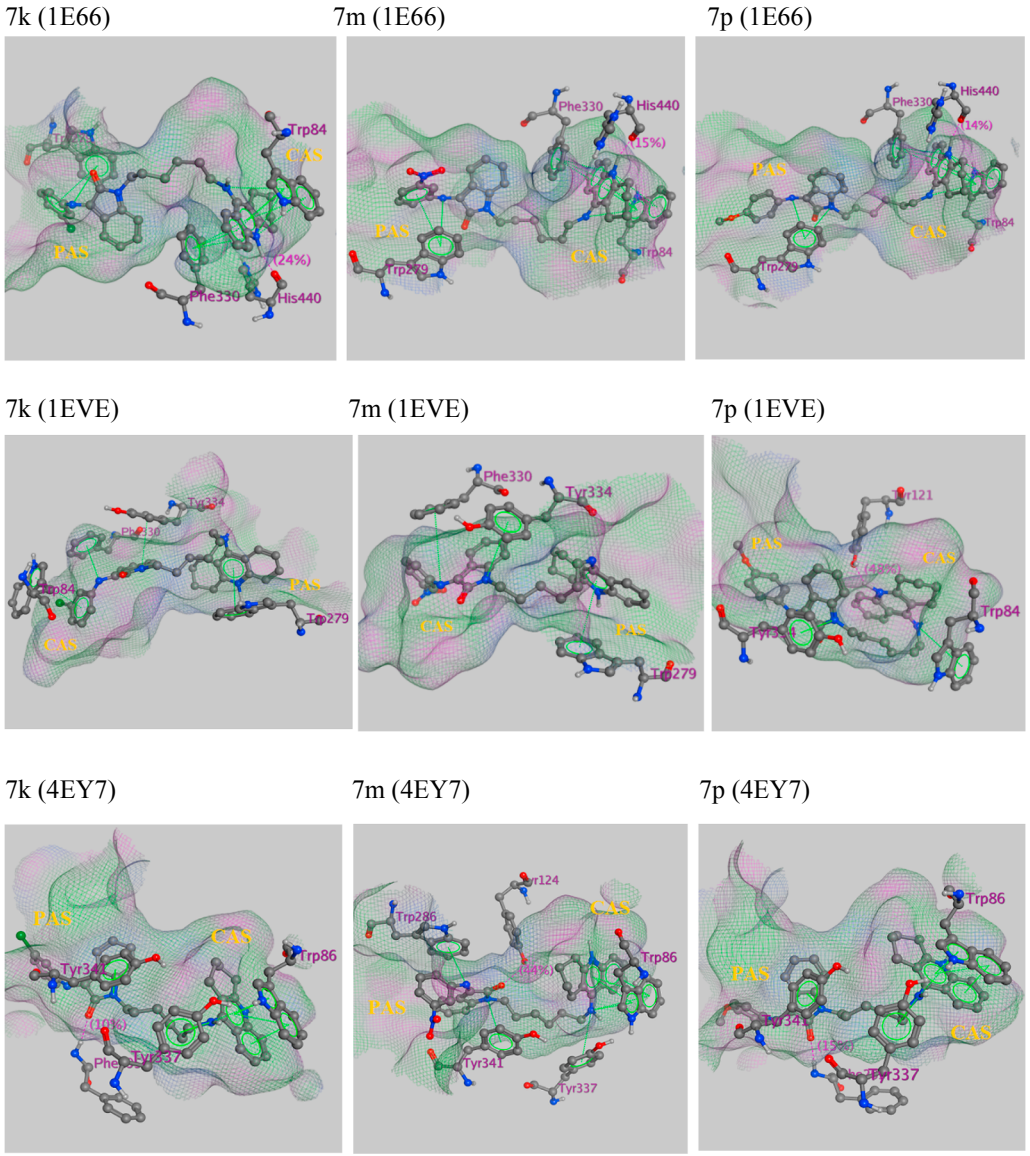

Fig. 2. The best pose of the most active compounds 7k, 7m and 7p with different x-ray crystal extructures (PDB code: 1E66, 1EVE, 4EY7) in the active site of AChE; and the residues of the active site involved in ligand binding.

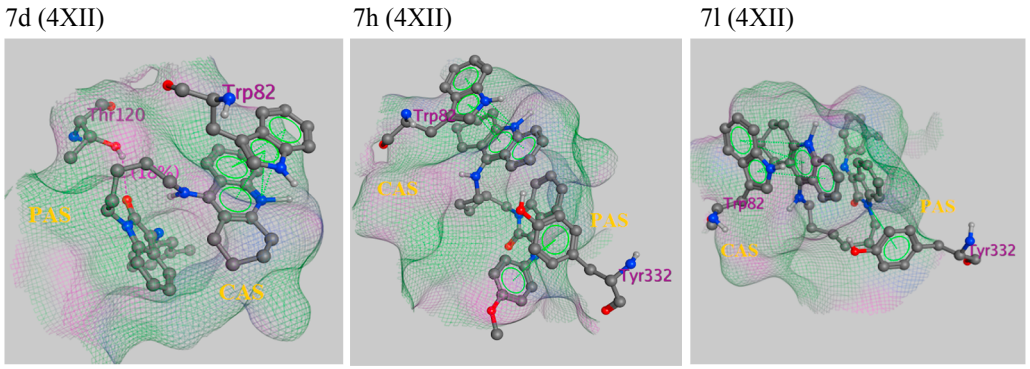

Fig.3. The best pose of the most active compounds 7d, 7h and 7l with x-ray crystal extructure (PDB code: 4XII) in the active site of BuChE; and the residues of the active site involved in ligand binding.

significant capacity to chelate ferrous ion with the value of 81% and 80%. It can be inferred that amino group conformation linked by tacrine to the spacer is the most efficient iron chelating site. 2-keto and 3-imine groups on isatin part of structures are also responsible for iron chelation. The high affinity of tacrine isatin Schiff base derivatives to ferrous ion is of great significance, because it was proposed that the transition metal ions contribute to the oxidative damage in neurodegenerative disorders such as Alzheimer's [57].

2.6. Inhibition of AChE-induced and self-induced Aβ aggregation

As several studies have found, AChE directly promotes pro-aggregation activity of Aβ protein into amyloid fibrils, and stabilizes the AChE–Aβ complex, which could cause neurotoxicity. This action likely happens through the interaction of Aβ with the PAS amino acid residues of AChE. Therefore, the inhibition of the PAS of AChE can help in prevention of Aβ aggregation and may turn AChEIs into potential disease modifying hybrids. The kinetic study of AChE inhibition and molecular modeling studies have demonstrated that our designed compounds could interact with the PAS as well as CAS of AChE. To further study of the dual action of tacrine-isatin Schiff base hybrid derivatives, the amyloid-beta protein ($A\beta_{1\text{-}40}$) anti-aggregating activity of **7k** and **7m**, as the most potent AChE inhibitors, was examined by a thioflavin-T fluorescent (ThT) assay. Two mentioned compounds were tested at 10 μM concentration and they were compared with donepezil as reference drug. The Aβ aggregation inhibition results are shown in Table 5.

From the results, it can be seen that both synthesized compounds exhibit a good inhibitory activity on AChE-induced $A\beta_{1\text{-}40}$ aggregation as well as donepezil. The results indicate that 7m (84.6% at 10 μM) is the potent inhibitor of Self-induced Aβ aggregation, which is 3.3-fold more potent than donepezil. The selected compounds exhibit very good activity in AChE-induced $A\beta_{1\text{-}40}$ aggregation thioflavin-T assay as well as self-induced $A\beta_{1\text{-}40}$ aggregation.

3. Conclusion

In conclusion, a series of tacrine–isatin Schiff base hybrid compounds were designed, synthesized and evaluated as novel multifunctional potent ChE inhibitors. Most of these compounds were potent ChEIs with IC_{50} values in the nanomolar range. Compounds 7k, 7m and

Table 4
Metal chelating percentage of synthesized compounds determined by a colorimetric method.

Compound	% of Fe^{2+} chelating at 400 μM
7a	64.95± 4.4
7b	74.47± 3.7
7c	78.93± 0.4
7d	77.63± 1.4
7e	46.37 ± 50.0
7f	73.68± 3.2
7g	74.94± 3.5
7h	46.33± 5.8
7i	74.45± 2.9
7j	43.15± 3.3
7k	81.52± 1.9
7l	73.38± 6.0
7m	33.51± 5.5
7n	72.42± 4.5
7o	64.06± 6.7
7p	80.24± 2.3
Tacrine	83.56± 1.0
EDTA	84.71± 0.9

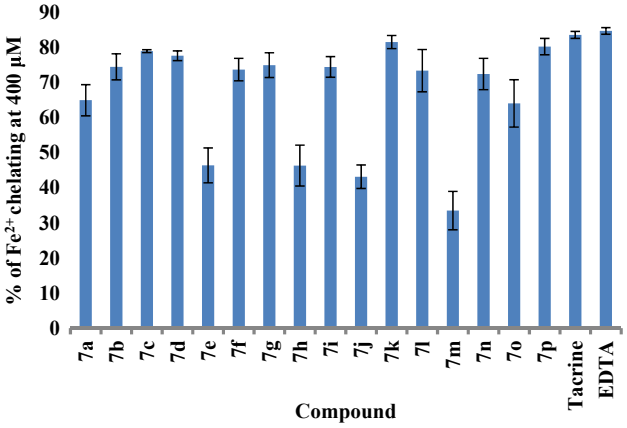

Fig. 4. Metal chelating activity of compounds 7a-p against EDTA as a standard iron chelator.

Table 3
RMSD values and binding energies of compounds 7k, 7m and 7p with the residues involved in the interactions.

PDB Code	RMSD of self-docking	Binding Energy (Kcal.mol^{-1})				7d		7 h		7 l		Tacrine
		7d	7 h	7 l	Tacrine	CAS	PAS	CAS	PAS	CAS	PAS	CAS
4XII	1.59	−11.8	−11.4	−11.5	−8.2	Trp82	Thr120	Trp82	Tyr332	Trp82	Tyr332	Trp82

Table 5
Inhibition of AChE-induced and self-induced A$\beta_{1\text{-}40}$ aggregation by compounds **7k** and **7m** using ThT method.

Compound	Inhibition of Aβ aggregation (%)	
	Self-induced[a]	AChE-induced[b]
7k***	n. d.[c]	79.1± 1.3
7m***	84.6± 3.3	70.8± 4.6
Donepezil***	25.6± 5.2	72.7± 1.2

[a] Inhibition of self-induced A$\beta_{1\text{-}40}$ aggregation (10 μM) produced by the tested compound at 10 μM concentration. Values are expressed as means±SEM of three experiments ($^{***}p < 0.0001$, compared to control).

[b] Co-aggregation inhibition of A$\beta_{1\text{-}40}$ and AChE by the tested compound at 10 μM concentration. Values are expressed as means±SEM of three experiments ($^{***}p < 0.0001$, compared to control).

[c] n. d. : not determined

7p were the most potent inhibitors, which were 92-, 62- and 41-fold, respectively, more active than that of the reference compound tacrine toward AChE. 7k also showed a potent BuChE inhibition but 7m and 7p exhibited selectivity for AChE over BuChE with the ratio of BuChE/AChE equal to 5.68 and 6.37, respectively. Amongst the hybrids, 7k with a chloro group in *meta*-position of the isatin Schiff base moiety and a six carbon linker between the two pharmacophores, delivered the best results with an IC_{50} value of 0.42 nM for AChE and 0.57 nM for BuChE. Kinetic studies of 7k and molecular modeling studies of all three compounds indicated that they were mixed-type inhibitors that simultaneously bind to active and peripheral sites of AChE. The molecular modeling studies further supported that 7m and 7p not only bind to CAS and PAS but also to the mid-gorge site of AChE. Meanwhile, 7k and 7m both exhibit a good inhibitory activity on AChE-induced and self-induced A$\beta_{1\text{-}40}$ aggregation, which confirmed the dual action of these compounds to bind to CAS and PAS of the enzyme. In addition, all three compounds represented good metal-chelating property in comparison with EDTA as the reference agent. Based on the results, compound 7k is a promising candidate to target ChEs with metal chelation activity for AD treatment. Furthermore, anti-aggregation activity of 7k and 7m qualified them as a potential multifunctional anti-AD drug candidate for further research. These candidate compounds have better cholinesterase inhibitory activity in compare with other studies including isatin Mannich bases [38], tacrine-melatonin derivatives [33], donepezil like indol derivatives [48] and benzylpyridinium-based benzoheterocycles [58].

4. Experimental section

4.1. Chemistry

Sixteen derivatives of tacrine-isatin Schiff base derivatives 7a-p were synthesized, shown in Scheme 2. All solvents and reagents were purchased either from Sigma or Merck Chemical Companies. All reaction progress was monitored by analytical thin layer chromatography (TLC) on precoated silica gel 60 GF_{254} sheets and the spots were detected under UV light (254 nm). Compound purification was performed by preparative chromatographic methods on silica gel, using either column chromatography (silica gel 60) or glass coated silica gel 60 GF_{254} plates. The ^1H NMR and ^{13}C NMR spectra were recorded in $CDCl_3$, and using TMS as the internal standard on a Brucker Avance DPX 500, 400, 300, 250 MHZ instrument. Chemical shifts are reported in ppm (δ), coupling constants reported in hertz (Hz), and all splitting patterns designed as s, singlet; d, doublet; t, triplet; m, multiplet; brs, broad singlet. Mass spectra were measured on Agilent Technology (HP) MS. Melting point was obtained on electrothermal 9200 instrument and uncorrected.

4.2. Synthesis and characterization

4.2.1. Synthesis of tacrine 2 (1,2,3,4-tetrahydroacridin-9-amine)

Tacrine **2** was prepared by the previously reported method with a slight modification. $AlCl_3$ (10 mmol) was added to the mixture of 2-aminobenzonitrile (10 mmol) and cyclohexanone (10 mmol) in toluene (50 mL) placed in a round bottom flask connected to a Dean-Stark water separator. The mixture was heated at reflux for 24 h under stirring. After cooling to room temperature, the suspension was filtered and the remaining solids were treated with NaOH solution (2 mol L^{-1}, 80 mL). Again, this mixture was heated at reflux for 24 h. On cooling to room temperature, the reaction mixture were extracted with ethylacetate (3 × 8 mL), the organic layers were combined and dried over anhydrous Na_2SO_4. The solvent was evaporated under reduced pressure to produce the desired product as a yellowish solid with 93% yield (mp: 180–185 °C).

^1H NMR ($CDCl_3$, 500 MHz) δ: 7.91 (d, 1H, J = 8.5 Hz), 7.70 (d, 1H, J = 7.5 Hz), 7.57 (t, 1H, J = 7.5 Hz), 7.36 (t, 1H, J = 7.5 Hz), 4.70 (s, 2H), 3.04 (t, 2H, J = 6.0 Hz), 2.61 (d, 1H, J = 6.3 Hz), 1.96–1.92 (m, 4H); ^{13}C NMR ($CDCl_3$, 500 MHz) δ: 158.76, 146.70, 146.58, 128.96, 128.63, 124.02, 119.81, 117.29, 110.56, 34.27, 23.92, 23.03, 22.94.

4.2.2. General procedure for the synthesis of 3a (N-(5-bromopentyl)-1,2,3,4-tetrahydroacridin-9-amine) and 3b (N-(6-bromohexyl)-1,2,3,4-tetrahydroacridin-9-amine)

A solution of dibromopentane or dibromohexane (15 mmol) in dry DMF (10 mL) was added to an ice-cold solution of tacrine **2** (1.0 g, 5.0 mmol) and NaH (15 mmol) in dry DMF (10 mL). Then the solution was stirred for 5 h at room temperature. When the reaction was completed (monitored by TLC), it was extracted with ethylacetate and water, followed by brine solution. The organic layer was dried over anhydrous Na_2SO_4 and concentrated under reduced pressure. Then the residue was purified by silica gel column chromatography using petroleum ether and ethyl acetate (100:50) as eluent to produce compounds **3a** and **3b** as brownish oil with 69.4% (3a) and 77.6% (3b) yields.

3b: ^1H NMR ($CDCl_3$, 300 MHz) δ: 8.62 (d, 1H, J = 8.7 Hz), 8.18 (d, 1H, J = 8.7 Hz), 7.73 (t, 1H, J = 7.7 Hz), 7.48 (t, 1H, J = 7.7 Hz), 4.10 (t, 1H, J = 6.5 Hz), 3.94 (t, 2H, J = 6.9 Hz), 3.45 (t, 1H, J = 6.5 Hz), 3.37 (t, 2H, J = 5.6 Hz), 2.62 (t, 2H, J = 5.3 Hz), 1.99–1.82 (m, 8H), 1.56–1.54 (m, 4H).

4.2.3. General procedure for the synthesis of isatin Schiff base derivatives 6a-6 h

Compounds 6a-h were prepared by reacting a mixture of isatin (25 mmol) and different substituted aromatic amines (25 mmol) in 30 mL of absolute ethanol containing 1.5 mL of glacial acetic acid. The reaction mixture was refluxed for about 3–5 h. The progress was monitored by TLC using petroleum ether/ ethyl acetate (2:1). The solvent was evaporated in vacuum and the yellow product was collected, and on recrystallization with petroleum ether gave the desired product 6a-6 h in reasonable yields.

6a: ^1H NMR ($CDCl_3$, 500 MHz) δ: 7.45 (t, 2H, J = 7.8 Hz), 7.31–7.25 (m, 2H), 7.05 (d, 2H, J = 7.5 Hz), 6.98 (d, 1H, J = 7.5 Hz), 6.74 (t, 1H, J = 7.8 Hz), 6.66 (d, 1H, J = 7.5 Hz); ^{13}C NMR ($CDCl_3$, 500 MHz) δ: 165.80, 154.92, 150.09, 145.96, 134.42, 129.45, 128.58, 126.28, 125.49, 122.74, 119.14, 117.93, 116.13, 112.07.

6f: ^1H NMR ($CDCl_3$, 500 MHz) δ: 7.43 (d, 2H, J = 8.5 Hz), 7.36 (t, 1H, J = 7.5 Hz), 7.02 (d, 2H, J = 8.5 Hz), 6.96 (d, 1H, J = 7.5 Hz), 6.82 (t, 1H, J = 7.8 Hz), 6.77 (d, 1H, J = 7.5 Hz); ^{13}C NMR ($CDCl_3$, 500 MHz) δ: 165.04, 154.96, 148.38, 145.75, 134.75, 131.00, 129.66, 128.73, 126.34, 122.96, 120.79, 119.53, 116.00, 111.91.

4.2.4. General procedure for the preparation of 7a-7p

Isatin Schiff base derivatives **6a-6 h** (3 mmol) were added to a stirred solution of anhydrous K_2CO_3 (6 mmol) in dry DMF (10 mL)

under N_2 atmosphere. Then, **3a** or **3b** (2.55 mmol) dissolved in dry DMF (10 mL), was added dropwise and the resulting dark red solution was stirred overnight at room temperature. The DMF was eliminated by washing it with water and extracted with ethyl acetate (50 mL ×3). The combined organic extracts were washed with brine solution and dried over anhydrous Na_2SO_4. The solvent was evaporated under reduced pressure and the residue was prepurified by silica gel column chromatography using petroleum ether/ ethyl acetate (100:25) as the mobile phase. To obtain purified target compounds **7a-p**, plate chromatography was performed using $CHCl_3$/MeOH (150:25) as eluent mixtures of solvents.

4.2.4.1. 3-(phenylimino)-1-(5-((1,2,3,4-tetrahydroacridin-9-yl)amino) pentyl)indolin-2-one (7a). Compound **3a** was treated with 3-(phenylimino)indolin-2-one (**6a**) according to general procedure to produce the desired product **7a** as an orange solid (Yield: 65.8%, mp 74–84 °C).

^{1}H NMR ($CDCl_3$, 250 MHz) δ: 8.00–7.94 (m, 2H), 7.51 (t, 1H, J = 7.6 Hz), 7.36 (t, 2H, J = 7.8 Hz), 7.29–7.22 (m, 2H), 7.20–7.18 (m, 1H), 6.92 (d, 2H, J = 8.3 Hz), 6.75 (d, 1H, J = 8 Hz), 6.68 (t, 1H, J = 7.6 Hz), 6.55 (d, 1H, J = 7.8 Hz), 3.76 (t, 2H, J = 6.9 Hz), 3.59 (t, 2H, J = 7.1 Hz), 3.04 (brs, 2H), 2.59 (brs, 2H), 1.81–1.79 (m, 4H),1.75–1.69 (m, 4H), 1.52–1.43 (m, 2H); ^{13}C NMR ($CDCl_3$, 400 MHz) δ: 163.41, 155.04, 154.36, 152.95, 150.27, 147.20, 143.15, 134.20, 130.08, 129.48, 129.27, 126.37, 125.39, 124.70, 124.33, 123.52, 122.70, 118.15, 117.70, 115.75, 115.11, 113.54, 109.49, 48.65, 39.74, 31.07, 30.85, 27.07, 24.54, 24.11, 24.316, 22.54, 21.75; MS *m/z* (%): 488.6 [M^+] (83.74), 413.6 (41.51), 398.6 (1.81), 291.4 (1.37), 277.4 (0.79), 267.5 (11.00), 263.5 (1.90), 225.4 (36.60), 221.4 (8.87), 211.4 (1 0 0), 197.4 (31.94), 93.3 (44.01), 77.3 (34.11).

4.2.4.2. 3-((2-chlorophenyl)imino)-1-(5-((1,2,3,4-tetrahydroacridin-9 yl) amino)pentyl)indolin-2-one (7b). Compound **3a** was treated with 3-((2-chlorophenyl)imino)indolin-2-one (**6b**) according to general procedure to produce the desired product **7b** as an orange solid (Yield: 75.8%; mp: 78–89 °C). ^{1}H NMR ($CDCl_3$, 300 MHz) δ: 8.23 (d, 1H, J = 8.1 Hz), 8.13 (d, 1H, J = 8.4 Hz), 7.53 (t, 1H, J = 7.4 Hz), 7.41 (d, 1H, J = 7.8 Hz), 7.36–7.25 (m, 3H), 7.14–7.09 (t, 1H, J = 7.4 Hz), 6.88 (d, 1H, J = 7.8 Hz), 6.81 (d, 1H, J = 7.8 Hz), 6.71 (t, 1H, J = 7.5 Hz), 6.43 (d, 1H, J = 7.5 Hz), 6.00 (brs, 1H, H_{NH}), 3.79–3.74 (m, 4H), 3.12 (brs, 2H), 2.63 (brs, 2H), 1.87–1.77 (m, 8H), 1.50–1.48 (m, 2H); ^{13}C NMR ($CDCl_3$, 300 MHz) δ: 163.07, 155.88, 154.54, 152.75, 147.29, 147.16, 140.68, 134.81, 131.28, 130.32, 129.52, 127.82, 126.14, 124.82, 124.10, 123.75, 123.07, 122.29, 118.83, 116.84, 116.06, 112.22, 109.63, 48.43, 39.67, 30.39, 29.68, 27.00, 24.28, 24.00, 22.23, 21.14;

MS *m/z* (%): 522.6 [M^+] (43.62), 487.6 (1.16), 413.5 (28.26), 396.5 (1.04), 326.5 (3.82), 311.3 (0.51), 297.4 (0.51), 267.5 (10.43), 255.3 (3.35), 225.4 (27.74), 211.4 (1 0 0), 197.3 (30.50), 127.3 (16.69), 111.3 (6.68).

4.2.4.3. 3-((3-chlorophenyl)imino)-1-(5-((1,2,3,4-tetrahydroacridin-9-yl) amino)pentyl)indolin-2-one (7c). Compound **3a** was treated with 3-((3-chlorophenyl)imino)indolin-2-one (**6c**) according to general procedure to produce the desired product **7c** as a yellow solid (Yield: 77.3%, mp: 100–110 °C). ^{1}H NMR ($CDCl_3$, 300 MHz) δ: 8.23 (d, 1H, J = 6.0 Hz), 8.04 (d, 1H, J = 7.2 Hz), 7.59–7.56 (m, 1H), 7.37–7.28 (m, 3H), 7.20–7.18 (m, 1H), 6.93 (s, 1H), 6.80–6.72 (m, 3H), 6.58 (d, 1H, J = 6.9 Hz), 5.05 (brs, 1H, H_{NH}), 3.78–3.74 (m, 4H), 3.14 (brs, 2H), 2.59 (brs, 2H), 1.82 (m, 8H), 1.51–1.47 (m, 2H); ^{13}C NMR ($CDCl_3$, 300 MHz) δ: 172.86, 169.40, 157.64, 154.86, 153.70, 151.35, 147.32, 142.03, 137.55, 135.25, 134.61, 131.47, 130.72, 128.05, 126.51, 125.31, 124.78, 123.59, 122.93, 117.84, 115.91, 115.52, 109.58, 48.78, 44.95, 39.59, 30.57, 30.24, 26.98, 24.17, 23.98, 22.33; MS *m/z* (%): 522.6 [M^+] (1 0 0), 487.6 (0.52), 411.6 (7.11), 398.6 (1.68), 325.5 (0.71), 311.4 (1.02), 297.4 (0.58), 267.5 (11.06), 255.3 (5.20), 225.4 (31.75), 211.4 (82.30), 197.4 (25.23), 127.3 (56.41), 111.3 (15.84).

4.2.4.4. 1-(5-((1,2,3,4-tetrahydroacridin-9-yl)amino)pentyl)-3-(m-tolylimino)indolin-2-one (7d). Compound **3a** was treated with 3-(m-tolylimino)indolin-2-one (**6d**) according to general procedure to produce the desired product **7d** as a yellow solid (Yield: 81.2%, mp: 98–104 °C).

^{1}H NMR ($CDCl_3$, 300 MHz) δ: 8.07 (d, 1H, J = 8.4 Hz), 8.02 (d, 1H, J = 8.4 Hz), 7.51 (t, 1H, J = 6.3 Hz), 7.31 (t, 1H, J = 7.7 Hz), 7.23 (t, 2H, J = 7.5 Hz), 6.98 (d, 1H, J = 7.2 Hz), 6.77 (d, 1H, J = 7.5 Hz), 6.71 (s, 1H), 6.71–6.66 (m, 2H), 6.57 (d, 1H, J = 7.5 Hz), 5.16 (brs, 1H, H_{NH}), 3.77–3.73 (brs, 2H), 3.648 (brs, 2H), 3.06 (brs, 2H), 2.62 (brs, 2H), 2.29 (s, 3H), 1.80–1.69 (m, 8H), 1.48–1.46 (m, 2H); ^{13}C NMR ($CDCl_3$, 300 MHz) δ: 163.45, 154.98, 154.16, 153.01, 150.29, 147.10, 143.27, 143.24, 139.41, 134.06, 130.15, 129.27, 126.37, 126.09, 124.81, 124.41, 123.57, 122.67, 118.15, 115.78, 114.57, 113.75, 109.42, 48.75, 39.66, 31.35, 30.72, 27.03, 24.51, 24.06, 22.53, 21.77, 21.48; MS *m/z* (%): 502.6 [M^+] (1 0 0), 413.5 (13.35), 305.4 (2.45), 267.4 (10.07), 237.4 (9.19), 225.4 (29.50), 211.4 (86.74), 197.3 (25.29), 106.3 (15.48), 91.3 (29.47).

4.2.4.5. 3-((3-nitrophenyl)imino)-1-(5-((1,2,3,4-tetrahydroacridin-9-yl) amino)pentyl)indolin-2-one (7e). Compound **3a** was treated with 3-((3-nitrophenyl)imino)indolin-2-one (**6e**) according to general procedure to produce the desired product **7e** as an orange solid (Yield: 64.2%, mp: 65–70 °C). ^{1}H NMR ($CDCl_3$, 300 MHz) δ: 8.23–8.21 (brs, 1H), 8.11 (d, 1H, J = 8.4 Hz), 8.04 (d, 1H, J = 7.8 Hz), 7.79 (s, 1H), 7.57–7.54 (m, 2H), 7.42 (t, 1H, J = 7.8 Hz), 7.33 (t, 1H, J = 7.4 Hz), 7.26 (d, 1H, J = 7.5 Hz), 6.85 (d, 1H, J = 8.1 Hz), 6.70 (t, 1H, J = 7.1 Hz), 6.45 (d, 1H, J = 7.2 Hz), 5.80 (brs, 1H, H_{NH}), 3.79–3.59 (m, 4H), 3.12 (brs, 2H), 2.62 (brs, 2H), 1.77 (brs, 8H), 1.50 (brs, 2H); ^{13}C NMR ($CDCl_3$, 300 MHz) δ: 162.89, 155.74, 154.33, 151.12, 149.08, 147.69, 135.27, 134.85, 131.18, 130.66, 126.22, 125.06, 124.79, 124.12, 123.60, 122.97, 119.97, 117.01, 115.21, 112.94, 112.38, 110.04, 109.30, 48.43, 39.78, 30.53, 29.87, 26.97, 24.29, 24.01, 22.26, 21.21; MS *m/z* (%): 533.6 [M^+] (65.45), 413.5 (18.08), 399.5 (1.44), 322.4 (0.47), 267.2 (13.93), 252.3 (11.49), 225.4 (27.27), 211.4 (1 0 0), 197.4 (28.88), 138.3 (59.42).

4.2.4.6. 3-((4-chlorophenyl)imino)-1-(5-((1,2,3,4-tetrahydroacridin-9-yl) amino)pentyl)indolin-2-one (7f). Compound **3a** was treated with 3-((4-chlorophenyl)imino)indolin-2-one (**6f**) according to general procedure to produce the desired product **7f** as a red solid (Yield: 76.4%, mp: 79–85 °C).

^{1}H NMR ($CDCl_3$, 250 MHz) δ: 8.03–8.00 (m, 2H), 7.59 (t, 1H, J = 7.6 Hz), 7.33 (d, 1H, J = 6.8 Hz), 7.39 (t, 2H, J = 7.6 Hz), 6.98 (d, 2H, J = 6.4 Hz), 6.86–6.81 (m, 2H), 6.74 (d, 1H, J = 6.8 Hz), 3.84 (t, 2H, J = 7.0 Hz), 3.60 (t, 2H, J = 7.0 Hz), 3.12 (brs, 2H), 2.72 (brs, 2H), 1.94–1.92 (m, 4H), 1.82–1.78 (m, 4H), 1.59–1.52 (m, 2H); ^{13}C NMR ($CDCl_3$, 400 MHz) δ: 163.13, 157.36, 154.73, 151.43, 148.62, 147.43, 145.94, 134.49, 130.84, 129.67, 129.03, 128.71, 127.43, 126.35, 124.03, 122.96, 122.75, 120.71, 119.39, 116.23, 115.60, 109.56, 108.92, 49.08, 39.87, 33.00, 31.16, 27.11, 24.72, 24.21, 22.88, 22.43; MS *m/z* (%): 522.6 [M^+] (81.04), 413.6 (23.00), 399.6 (1.25), 325.4 (0.63), 311.4 (0.74), 297.4 (0.81), 267.5 (12.11), 225.3 (5.39), 225.4 (36.41), 211.4 (1 0 0), 197.4 (31.05), 127.3 (81.14), 111.3 (13.79).

4.2.4.7. 1-(5-((1,2,3,4-tetrahydroacridin-9-yl)amino)pentyl)-3-(p-tolylimino)indolin-2-one (7 g). Compound **3a** was treated with 3-(p-tolylimino)indolin-2-one (**6 g**) according to general procedure to produce the desired product **7g** as an orange solid (Yield: 78.6%, mp: 116–122 °C).

^{1}H NMR ($CDCl_3$, 500 MHz) δ: 8.04 (d, 1H, J = 8.5 Hz), 8.00 (d, 1H, J = 8.5 Hz), 7.52 (t, 1H, J = 7.5 Hz), 7.35–7.30 (m, 2H), 7.20 (d, 2H,

J = 8.0 Hz), 6.89 (d, 2H, *J* = 8.0 Hz), 6.82 (d, 1H, *J* = 8.0 Hz), 6.74–6.74 (m, 2H), 3.79 (t, 2H, *J* = 7.0 Hz), 3.65 (t, 2H, *J* = 7.0 Hz), 3.058 (brs, 2H), 2.643 (brs, 2H), 2.379 (s, 3H),1.83–1.74 (m, 8H), 1.53–1.47 (m, 2H); ^{13}C NMR ($CDCl_3$, 500 MHz) *δ*: 163.44, 155.39, 154.06, 152.63, 147.55, 147.09, 143.66, 135.19, 134.00, 129.95, 129.78, 129.09, 126.16, 125.10, 124.20, 123.44, 122.56, 118.41, 117.92, 115.81, 115.21, 113.88, 109.41, 48.64, 39.70, 31.43, 30.86, 27.05, 24.60, 24.10, 22.57, 21.86, 21.05; MS *m/z* (%): 502 [M^+] (83.37), 413 (47.83), 225 (35.05), 211 (1 0 0), 197 (32.02), 183 (19.72), 106 (76.36).

4.2.4.8. 3-((4-methoxyphenyl)imino)-1-(5-((1,2,3,4-tetrahydroacridin-9-yl)amino)pentyl)indolin-2-one (7h). Compound **3a** was treated with 3-((4-methoxyphenyl)imino)indolin-2-one (**6 h**) according to general procedure to produce the desired product **7h** as a red solid (Yield: 80.7%, mp: 78–83 °C). ^{1}H NMR ($CDCl_3$, 400 MHz) *δ*: 8.25 (d, 1H, *J* = 8.4 Hz), 8.12 (d, 1H, *J* = 8.4 Hz), 7.63 (t, 1H, *J* = 7.2 Hz), 7.42 (t, 1H, *J* = 7.2 Hz), 7.37 (t, 1H, *J* = 7.6 Hz), 7.06–6.98 (m, 5H), 6.87 (d, 1H, *J* = 8.0 Hz), 6.82 (t, 1H, *J* = 7.2 Hz), 3.89 (s, 3H), 3.87–3.85 (m, 2H), 3.78 (t, 2H, *J* = 6.4 Hz), 3.20(t, 2H, *J* = 6.0 Hz), 2.69 (t, 2H, *J* = 6.0 Hz), 1.93–1.80 (m, 8H), 1.61–1.53 (m, 2H); ^{13}C NMR ($CDCl_3$, 400 MHz) *δ*: 163.67, 157.90, 154.29, 153.71, 153.52, 147.02, 142.93, 142.44, 133.97, 130.54, 125.82, 124.54, 124.09, 123.74, 123.23, 122.62, 120.16, 117.73, 115.90, 114.59, 113.63, 113.21, 109.47, 48.69, 39.62, 30.79, 30.65, 29.71, 27.04, 24.41, 24.05, 22.45, 21.58; MS *m/z* (%): 518.7 [M^+] (94.84), 413.6 (24.88), 265.5 (10.95), 253.5 (9.19), 251.4 (10.66), 225.4 (31.44), 211.4 (1 0 0), 197.4 (26.33), 123.3 (27.44), 108.3 (38.71).

4.2.4.9. 3-(phenylimino)-1-(6-((1,2,3,4-tetrahydroacridin-9-yl)amino) hexyl)indolin-2-one (7i). Compound **3b** was treated with 3-(phenylimino)indolin-2-one (**6a**) according to general procedure to produce the desired product **7i** as a dark orange solid (Yield: 77.1%, mp: 97–102 °C). ^{1}H NMR ($CDCl_3$, 500 MHz) *δ*: 7.93 (d, 1H, *J* = 8.5 Hz), 7.88 (d, 1H, *J* = 8.0 Hz), 7.50 (t, 1H, *J* = 8.0 Hz), 7.39 (t, 2H, *J* = 8.5 Hz), 7.32–7.27 (m, 2H), 7.21 (t, 1H, *J* = 7.5 Hz), 6.97 (d, 2H, *J* = 7.5 Hz), 6.78 (d, 1H, *J* = 8.0 Hz), 6.70 (t, 1H, *J* = 7.5 Hz), 6.59 (d, 1H, *J* = 7.5 Hz), 3.74 (t, 2H, *J* = 7.3 Hz), 3.45 (t, 2H, *J* = 7.3 Hz), 3.03 (brs, 2H), 2.68 (brs, 2H), 1.88–1.87 (m, 4H),1.72–1.66 (m, 2H), 1.66–1.61 (m, 2H), 1.42–1.40 (m, 4H); ^{13}C NMR ($CDCl_3$, 500 MHz) *δ*: 163.18, 158.42, 154.39, 150.70, 150.30, 147.40, 147.33, 134.07, 129.403, 128.62, 128.51, 128.24, 126.28, 125.28, 123.60, 122.81, 122.51, 120.24, 119.01, 117.70, 115.98, 115.71, 109.42, 49.26, 39.93, 33.97, 31.60, 27.23, 26.61, 26.56, 24.81, 23.03, 22.76; MS *m/z* (%): 502.7 [M^+] (83.00), 427.6 (13.6), 225.4 (29.44), 211.4 (1 0 0), 197.4 (29.09), 182.4 (17.34), 77.4 (30.31).

4.2.4.10. 3-((2-chlorophenyl)imino)-1-(6-((1,2,3,4-tetrahydroacridin-9-yl)amino)hexyl)indolin-2-one (7j). Compound **3b** was treated with 3-((2-chlorophenyl)imino)indolin-2-one (**6b**) according to general procedure to produce the desired product **7j** as a yellow solid (Yield: 72.5%, mp: 106–110 °C). ^{1}H NMR ($CDCl_3$, 400 MHz) *δ*: 8.24 (d, 1H, *J* = 8.4 Hz), 8.12 (d, 1H, *J* = 8.4 Hz), 7.64 (t, 1H, *J* = 7.6 Hz), 7.52 (d, 1H, *J* = 7.6 Hz), 7.45–7.34 (m, 3H), 7.22 (t, 1H, *J* = 7.6 Hz), 7.00 (d, 1H, *J* = 8.8 Hz), 6.89 (d, 1H, *J* = 8.0 Hz), 6.81 (t, 1H, *J* = 7.6 Hz), 6.55 (d, 1H, *J* = 7.6 Hz), 3.84 (t, 2H, *J* = 7.0 Hz), 3.78 (t, 2H, *J* = 7.0 Hz), 3.21 (t, 2H, *J* = 6.0 Hz), 2.69 (t, 2H, *J* = 6.0 Hz), 1.93–1.88 (m, 4H), 1.83–1.78 (t, 4H), 1.54–1.50 (m, 4H); ^{13}C NMR ($CDCl_3$, 400 MHz) *δ*: 162.96, 155.91, 147.34, 134.70, 134.50, 130.72, 130.35, 129.52, 127.80, 127.05, 126.18, 126.12, 125.37, 124.59, 123.85, 123.61, 123.46, 122.99, 122.38, 118.89, 116.14, 109.56, 109.14, 48.68, 39.83, 31.29, 29.73, 27.14, 26.36, 26.20, 24.17, 22.40, 21.55; MS *m/z* (%): 536.6 [M^+] (54.98), 427.6 (30.58), 297.4 (1.59), 281.5 (6.01), 255.3 (3.69), 225.4 (25.47), 211.4 (1 0 0), 197.4 (27.77), 127.3 (49.76), 111.3 (7.21).

4.2.4.11. 3-((3-chlorophenyl)imino)-1-(6-((1,2,3,4-tetrahydroacridin-9-yl)amino)hexyl)indolin-2-one (7k). Compound **3b** was treated with 3-((3-chlorophenyl)imino)indolin-2-one (**6c**) according to general procedure to produce the desired product **7k** as a yellow solid (Yield: 78.9%, mp: 90–95 °C). ^{1}H NMR ($CDCl_3$, 300 MHz) δ: 8.21 (d, 1H, *J* = 8.4 Hz), 8.05 (d, 1H, *J* = 8.7 Hz), 7.56 (t, 1H, *J* = 7.4 Hz), 7.36–7.27 (m, 3H), 7.17–7.14 (m, 1H), 6.93 (s, 1H), 6.80 (d, 2H, *J* = 7.8 Hz), 6.73 (t, 1H, *J* = 7.7 Hz), 6.56 (d, 1H, *J* = 7.2 Hz), 5.16 (brs, 1H, H_{NH}), 3.76–3.68 (m, 4H), 3.13 (brs, 2H), 2.60 (brs, 2H), 1.82 (brs, 4H), 1.75–1.64 (m, 4H), 1.43–1.42 (m, 4H); ^{13}C NMR ($CDCl_3$, 300 MHz) *δ*: 163.073, 154.991, 153.778, 151.407, 147.489, 135.199, 134.596, 131.20, 130.85, 130.70, 129.66, 126.47, 125.25, 124.75, 124.65, 123.68, 123.53, 122.81, 118.77, 117.86, 115.95, 115.50, 109.65, 48.61, 39.78, 31.20, 30.43, 27.10, 26.33, 26.18, 24.14, 22.34, 21.43; MS *m/z* (%): 536.6 [M^+] (71.79), 427.6 (11.63), 413.6 (0.76), 281.5 (4.91), 255.3 (3.96), 225.4 (24.58), 211.4 (1 0 0), 197.4 (24.22), 127.3 (10.83), 111.3 (12.26).

4.2.4.12. 1-(6-((1,2,3,4-tetrahydroacridin-9-yl)amino)hexyl)-3-(m-tolylimino)indolin-2-one (7l). Compound **3b** was treated with 3-(m-tolylimino)indolin-2-one (**6d**) according to general procedure to produce the desired product **7l** as an orange solid (Yield: 79.6%, mp: 94–101 °C). ^{1}H NMR ($CDCl_3$, 300 MHz) *δ*: 8.23 (d, 1H, *J* = 7.8 Hz), 8.15 (d, 1H, *J* = 8.4 Hz), 7.61–7.56 (t, 1H, *J* = 7.5 Hz), 7.41–7.25 (m, 3H), 7.03 (d, 1H, *J* = 7.5 Hz), 6.84 (d, 1H, *J* = 7.8 Hz), 6.78 (s, 1H), 6.78–6.71 (m, 2H), 6.62 (d, 1H, *J* = 7.5 Hz), 3.78 (t, 2H, *J* = 6.8 Hz), 3.16 (brs, 2H), 2.69 (brs, 2H), 2.35 (s, 1H), 1.86–1.71 (m, 8H), 1.47 (m, 4H); ^{13}C NMR ($CDCl_3$, 300 MHz) *δ*: 163.33, 154.23, 153.95, 153.64, 150.30, 147.20, 141.78, 139.38, 134.04, 130.78, 129.25, 126.33, 126.05, 124.56, 123.89, 123.43, 122.59, 118.15, 117.40, 115.76, 114.57, 112.77, 109.46, 48.42, 39.75, 31.08, 30.37, 27.13, 26.35, 26.21, 24.30, 22.35, 21.46, 21.41; MS *m/z* (%): 516.7 [M^+] (87.20), 427.6 (5.83), 413.7 (0.74), 319.5 (2.50), 306.5 (0.90), 291.5 (0.42), 281.5 (3.95), 267.5 (22.28), 237.5 (7.71), 225.5 (22.21), 211.5 (1 0 0), 197.5 (24.95), 106.4 (36.33), 91.4 (36.09).

4.2.4.13. 3-((3-nitrophenyl)imino)-1-(6-((1,2,3,4-tetrahydroacridin-9-yl) amino)hexyl)indolin-2-one (7m). Compound **3b** was treated with 3-((3-nitrophenyl)imino)indolin-2-one (**6e**) according to general procedure to produce the desired product **7m** as an orange solid (Yield: 67.8%, mp: 74–80 °C). ^{1}H NMR ($CDCl_3$, 300 MHz) *δ*: 8.32 (brs, 1H), 8.22 (d, 1H, *J* = 8.4 Hz), 8.15–8.07 (m, 1H), 7.83 (s, 1H), 7.62–7.59 (m, 2H), 7.48–7.30 (m, 3H), 6.90 (d, 1H, *J* = 8.1 Hz), 6.75–6.73 (m, 1H), 6.49 (d, 1H, *J* = 6.6 Hz), 6.27 (brs, 1H, H_{NH}), 3.87–3.62 (m, 4H), 3.19 (brs, 2H), 2.70–2.61 (m, 2H), 1.84–1.66 (m, 8H), 1.48 (brs, 4H); ^{13}C NMR ($CDCl_3$, 300 MHz) *δ*: 162.75, 155.82, 154.79, 151.13, 149.03, 147.79, 146.36, 140.34, 135.25, 131.45, 130.65, 129.43, 126.18, 124.79, 124.14, 122.87, 119.91, 116.66, 115.16, 113.87, 112.94, 111.94, 110.07, 48.22, 39.91, 30.96, 29.44, 27.08, 26.33, 26.16, 24.18, 22.17, 21.06; MS *m/z* (%): 547.7 [M^+] (10.69), 427.6 (38.43), 413.6 (1.44), 336.5 (0.59), 281.5 (4.50), 267.5 (12.06), 225.4 (17.91), 211.4 (83.48), 197.4 (31.34), 138.3 (1 0 0), 122.3 (1.02), 46.3 (6.71).

4.2.4.14. 3-((4-chlorophenyl)imino)-1-(6-((1,2,3,4-tetrahydroacridin-9-yl)amino)hexyl)indolin-2-one (7n). Compound **3b** was treated with 3-((4-chlorophenyl)imino)indolin-2-one (**6f**) according to general procedure to produce the desired product **7n** as an orange solid (Yield: 78.4%, mp: 96–104 °C). ^{1}H NMR ($CDCl_3$, 500 MHz) *δ*: 7.97 (d, 1H, *J* = 8.5 Hz), 7.94 (d, 1H, *J* = 8.5 Hz), 7.55 (t, 1H, *J* = 7.5 Hz), 7.40 (d, 2H, *J* = 8.5 Hz), 7.38–7.33 (m, 2H), 6.96 (d, 2H, *J* = 8.5 Hz), 6.84 (d, 1H, *J* = 8.0 Hz), 6.79 (t, 1H, *J* = 7.5 Hz), 6.70 (d, 1H, *J* = 7.5 Hz), 3.78 (t, 2H, *J* = 7.0 Hz), 3.52 (t, 2H, *J* = 7.0 Hz), 3.08 (brs, 2H), 2.70 (brs, 2H), 1.91–1.90 (m, 4H), 1.76–1.66 (m, 4H), 1.47–1.43 (m, 4H); ^{13}C NMR ($CDCl_3$, 500 MHz) *δ*: 163.00, 157.87, 154.78, 151.08, 148.63, 147.53, 146.65, 134.43, 130.74, 129.61, 128.66, 128.62, 128.01, 126.28, 123.77, 123.24, 122.90, 122.63, 120.65, 119.86, 119.37,

115.56, 109.58, 49.19, 39.97, 33.47, 31.59, 27.22, 26.59, 26.53, 24.75, 22.95, 22.59; MS *m/z* (%): 536.6 [M^+] (85.80), 427.6 (8.86), 281.4 (5.53), 267.5 (25.23), 225.4 (27.19), 211.4 (1 0 0), 197.4 (27.90), 182.4 (18.69), 127.3 (92.26).

4.2.4.15. 1-(6-((1,2,3,4-tetrahydroacridin-9-yl)amino)hexyl)-3-(p-tolylimino)indolin-2-one (7o). Compound **3b** was treated with 3-(p-tolylimino)indolin-2-one (**6 g**) according to general procedure to produce the desired product **7o** as an orange solid (Yield: 79.2%, mp: 96–101 °C). ^{1}H NMR ($CDCl_3$, 500 MHz) *δ*: 7.99–7.96 (m, 2H), 7.56 (t, 1H, *J* = 7.8 Hz), 7.37–7.31 (m, 2H), 7.23 (d, 2H, *J* = 8.0 Hz), 6.92 (d, 2H, *J* = 8.5 Hz), 6.83 (d, 1H, *J* = 8.0 Hz), 6.77–6.76 (m, 2H), 4.93 (brs, 1H, H_{NH}), 3.79 (t, 2H, *J* = 7 Hz), 3.55 (t, 2H, *J* = 7.25 Hz), 3.09 (brs, 2H), 2.70 (brs, 2H), 2.41 (s, 3H), 1.92–1.91 (m, 4H), 1.77–1.66 (m, 4H), 1.47–1.42 (m, 4H); ^{13}C NMR ($CDCl_3$, 500 MHz) *δ*: 163.33, 157.5, 157.46, 154.09, 151.38, 147.62, 147.27, 146.17, 135.13, 133.86, 129.93, 129.11, 128.82, 127.52, 126.18, 123.83, 122.97, 122.44, 119.61, 117.96, 115.88, 115.22, 109.33, 49.13, 39.88, 33.05, 31.56, 27.22, 26.57, 26.51, 24.70, 22.88, 22.47, 21.06; MS *m/z* (%): 516.6 [M^+] (1 0 0), 425.5 (4.84), 413.5 (6.32), 281.5 (4.36), 267.4 (18.10), 235.4 (7.32), 225.4 (21.70), 211.4 (75.92), 197.3 (23.00), 182.3 (14.98), 167.3 (9.19), 106.3 (41.80), 91.3 (22.37).

4.2.4.16. 3-((4-methoxyphenyl)imino)-1-(6-((1,2,3,4-tetrahydroacridin-9-yl)amino)hexyl)indolin-2-one (7p). Compound **3b** was treated with 3-((4-methoxyphenyl)imino)indolin-2-one (**6 h**) according to general procedure to produce the desired product **7p** as a red solid (Yield: 74.8%, mp: 92–103 °C). ^{1}H NMR ($CDCl_3$, 300 MHz) *δ*: 8.20 (d, 1H, *J* = 7.2 Hz), 8.06 (d, 1H, *J* = 8.4 Hz), 7.54 (brs, 1H), 7.35–7.20 (m, 2H), 6.96–6.86 (m, 5H), 6.79 (d, 1H, *J* = 7.5 Hz), 6.71 (t, 1H, *J* = 7.5 Hz), 3.79 (s, 3H), 3.73 (brs, 2H), 3.71 (brs, 2H), 3.12 (brs, 2H), 2.61 (brs, 2H), 1.80 (m, 4H), 1.70–1.68 (m, 4H), 1.41 (m, 4H); ^{13}C NMR ($CDCl_3$, 300 MHz) *δ*: 168.71, 163.54, 157.86, 153.85, 153.82, 153.77, 149.11, 147.14, 142.98, 133.88, 130.84, 128.77, 125.80, 124.63, 123.80, 122.51, 120.12, 117.43, 115.90, 114.56, 113.59, 112.78, 109.45, 48.52, 39.69, 31.15, 30.40, 29.68, 27.14, 26.32, 26.18, 24.23, 22.33, 21.42; MS *m/z* (%): 532.6 [M^+] (56.49), 427.5 (22.37), 334.4 (1.82), 321.5 (0.57), 307.4 (0.36), 281.4 (4.75), 267.4 (21.35), 251.3 (5.70), 225.3 (25.47), 211.3 (1 0 0), 197.3 (25.40).

4.3. In vitro inhibition studies on AChE and BuChE

Acetylcholinesterase (AChE, E.C. 3.1.1.7, from electric eel), butyrylcholinesterase (BuChE, E.C. 3.1.1.8, from equine serum), 5, 5′-dithiobis-(2-nitrobenzoic acid) (Ellman's reagent, DTNB), acetylthiocholine iodide (ATI), butylthiocholine iodide (BTI), were purchased from Sigma Aldrich company. The inhibition capacity of the tested compounds 7a-p against AChE/BuChE was performed using colorimetric method assessed by Ellman et al. Tacrine and synthesized derivatives were dissolved in DMSO (40 mM). In a 24-well plate, 2000 µl of NaH_2PO_4/Na_2HPO_4 buffer (0.1 M, pH = 8), 60 µl of DTNB (0.01 M), 20 µl of AChE (1ku prepared in NaH_2PO_4/Na_2HPO_4 buffer (0.1 M) and glycerine 25%, pH = 8.0, 2 units/mL in 0.5 mL aliquots) or 20 µl of BuChE (1ku prepared in NaH_2PO_4/Na_2HPO_4 buffer (0.1 M) and glycerine 25%, pH = 8.0, 2 units/mL in 0.5 mL aliquots) were incubated with 30 µl in various concentrations of tested compounds (0.026–400 µM) at room temperature for 5 min. Afterward, 20 µl of the corresponding substrate acetylthiocholine iodide (0.15 M) or S-butyrylthiocholine iodide (0.15 M) was added and the absorbance was measured at 2 min intervals at a wavelength of 412 nm. The compound concentration produced 50% of enzyme activity inhibition (IC_{50}), was calculated by nonlinear regression analysis of the response–concentration (log) curve. Results are expressed as the mean ± SD of at least three different experiments performed in triplicate. All experiments were performed on a Synergy HTX Multi-Mode Reader-BioTek.

4.4. Kinetic study of AChE inhibition

Kinetic mechanism of AChE was carried out by Ellman's method in various concentrations (1.13, 2.22 and 4.32 nM) of selected compound 7k. In the Lineweaver–Burk plot (or double reciprocal plot), 1/ [velocity] was plotted against 1/ [substrate] at different concentrations of the substrate acetylthiocholine iodide (0.69, 1.37 and 3.38 mM). The plots were assessed by a weighted least-squares analysis that assumed the variance of velocity (v) to be a constant percentage of v for the entire data set. Slopes of these reciprocal plots were then plotted against the concentration of 7k in a weighted analysis, and Ki was determined as the intercept on the negative x-axis. Data analysis was performed with GraphPad Prism 4.03 software (GraphPad Software Inc.).

4.5. Metal chelating assay

The ferrous ion chelating power of the synthesized compounds was measured by the method of Dinis with a slight modification [56,59]. All experiments were performed in 24-well microplates. In each well, 100 µl of each synthetic compound (4 mM) prepared in methanol was incubated with 100 µl of $FeCl_2$ (0.6 mM) and 700 µl of methanol. The reaction was initiated by adding 100 µl of ferrozine (5 mM), which was shaken at room temperature for 10 min. Afterward, the absorbance at 562 nm was measured. Methanol, Fe^{2+} and ferrozine were used as a blank sample. For comparison of iron-chelating activity, EDTA was used as a standard iron chelator.

4.6. Inhibition of self-induced and AChE-Induced $A\beta_{1\text{-}40}$ aggregation assay

Inhibitory properties of compounds on self induced and AChE induced aggregation of amyloid *β* protein 1–40 was determined using a thioflavin T (ThT)-based fluorescence assay [60]. The ThT excitation/emission was measured at 448 nm/490 nm at 48 h using a multimode plate reader (BMG Labtech Omega FLUOstar). Amyloid *β* protein 1–40 (Sigma A1075) was dissolved in Phosphate Buffer Saline pH 7.4 (PBS, HyClone Thermo Scientific) containing 1% ammonium hydroxide. 12.5 µM Amyloid *β* protein 1–40 was incubated for 72 h at 37 °C for prefibrillation. For the assay $A\beta_{1\text{-}40}$ (10 µl) ± human recombinant AChE (0.01 u/ml, Sigma C1682) were added to 0.05 M KP buffer pH 7.4 and incubated at 37 °C for 48 h in the absence and presence of compounds (10 µM). Incubated mixture (100 µl) was mixed with 50 µl of thioflavin T (ThT, 200 µM) in 50 mM glycine-NaOH buffer (pH 8.5). Donepezil (10 µM, Sigma D-6821) were also tested as reference agent.

Inhibition percent of self or AChE-induced aggregation due to the presence of the tested compounds were determined by the following calculation: 100-[(IFi/IFo) × 100] where IFi and IFo are the fluorescence intensities obtained for A*β* ± AChE in the presence and in the absence of inhibitors. Statistical analysis was performed using GraphPad Prism software using one-way ANOVA analysis (Bonferroni's test) and *p*-Values < 0.05 were considered statistically significant.

4.7. Docking simulation method

Since different 3D-structures were released for AChE and BuChE, docking validation was used to select a proper x-ray structure for docking simulation. From these complexes, 19 PDB codes were selected from Protein Data Bank (http://www.rcsb.org). Five 3D X-ray crystal structures of the TcAChE, hAChE and fourteen 3D X-ray crystal structures of hBuChE were retrieved from Protein Data Bank (PDB) based on the similarity of cognate ligands with our compound structures in order to find the starting model of AChE and BuChE. The retrieved PDB codes for AChE were 2CKM, 2CMF, 1EVE, 4EY7 and 1E66. All the retrieved PDB codes were subjected to self-docking validation test. In this step, the cognate ligands were re-docked on their corresponding 3D structures and the best pose of docking was superimposed with the native

conformation of the ligand at crystallographic state. Amongst the pdb files of the receptors, 1E66 complexed with huprine, 1EVE and 4EY7 complexed with donepezil for AChE and 4XII complexed with nitroxoline for BuChE were selected based on root-mean-square deviation (RMSD) values as shown in Tables 2 and 3. The compound structures of 7k, 7m, 7p were sketched, energy minimized and the three ligand molecules were saved in pdbqt format. To prepare protein for docking simulation, all co-crystallized ligands and water molecules were removed and the missing hydrogens were added. Non-polar hydrogens were merged with their corresponding carbons and then the protein was converted into the required pdbqt format. All preparation was done using Auto Dock Tools package (1.5.6).

Cross-docking simulations were performed using bash scripting in linux operating system. Autodock Vina (1.1.2) was used for docking within a box defined by following parameters. The grid box with the size of 30× 30 × 30 was determined and the box was centered on co-crystalized ligand. The center of grid box was determined as [x = 3.62, y = 69.11, z = 64.75] for 1E66, [x = 5.16, y = 66.92, z = 66.42] for 1EVE, [x = −11.19, y = −46.35, z = 28.86] for 4EY7 and [x = 6.88, y = −15.86, z = -8.45] for 4XII. The exhaustiveness was set to 100 and the other docking parameters were set as default. At the end of cross-docking simulations, the best docking poses were selected for further analysis of enzyme-inhibitor interactions.

Acknowledgment

This article was extracted from the PhD dissertation (grant number: 94-7565) written by Elham Riazimontazer and approved by the Research Vice-Chancellor at Shiraz University of Medical Sciences. The authors wish to thank Mr. H. Argasi at the Research Consultation Center (RCC) of Shiraz University of Medical Sciences for his invaluable assistance in editing this manuscript.

References

[1] S.I. Cohen, P. Arosio, J. Presto, et al., A molecular chaperone breaks the catalytic cycle that generates toxic Aβ oligomers, Nat. Struct. Mol. Biol. 22 (2015) 207–213, https://doi.org/10.1038/nsmb.2971.
[2] S. Cohen. Samuel Cohen researches Alzheimer's disease and other neurodegenerative disorders, 2015. London: TED@BCG London, < https://www.ted.com/speakers/samuel_cohen > .
[3] A. Alzheimer's, 2015 Alzheimer's disease facts and figures, Alzheimers Dement 11, 2015, pp. 332–384. https://doi.org/10.1016/j.jalz.2015.02.003.
[4] C. Zhang, Q.-Y. Du, L.-D. Chen, et al., Design, synthesis and evaluation of novel tacrine-multialkoxybenzene hybrids as multi-targeted compounds against Alzheimer's disease, Eur. J. Med. Chem. 116 (2016) 200–209, https://doi.org/10.1016/j.ejmech.2016.03.077.
[5] S. Burmaoglu, A.O. Yilmaz, M.F. Polat, et al., Synthesis and biological evaluation of novel tris-chalcones as potent carbonic anhydrase, acetylcholinesterase, butyrylcholinesterase and α-glycosidase inhibitors, Bioorg. Chem. 85 (2019) 191–197, https://doi.org/10.1016/j.bioorg.2018.12.035.
[6] T. Arendt, Alzheimer's disease as a disorder of mechanisms underlying structural brain self-organization, Neuroscience 102 (2001) 723–765, https://doi.org/10.1016/S0306-4522(00)00516-9.
[7] C. Bayrak, P. Taslimi, H.S. Karaman, et al., The first synthesis, carbonic anhydrase inhibition and anticholinergic activities of some bromophenol derivatives with S including natural products, Bioorg. chem. 85 (2019) 128–139, https://doi.org/10.1016/j.bioorg.2018.12.012.
[8] D.R. Thal, K. Del Tredici, H. Braak, Neurodegeneration in normal brain aging and disease, Sci. Aging Knowledge Environ. 2004 (2004) pe26, https://doi.org/10.1126/sageke.2004.23.pe26.
[9] R. Crowther, M. Goedert, Abnormal tau-containing filaments in neurodegenerative diseases, J. Struct. Biol. 130 (2000) 271–279, https://doi.org/10.1006/jsbi.2000.4270.
[10] T.A. Bayer, O. Wirths, K. Majtényi, et al., Key factors in Alzheimer's disease: β-amyloid precursor protein processing, metabolism and intraneuronal transport, Brain Pathol. 11 (2001) 1–11, https://doi.org/10.1111/j.1750-3639.2001.tb00376.x.
[11] S.L. Cole, R. Vassar, The Alzheimer's disease β-secretase enzyme, BACE1, Mol. Neurodegener. 2 (2007) 22, https://doi.org/10.1186/1750-1326-2-22.
[12] L. Mucke, D.J. Selkoe, Neurotoxicity of amyloid β-protein: synaptic and network dysfunction, Cold Spring Harb, Perspect. Med. (2012) 1–17, https://doi.org/10.1101/cshperspect.a006338.
[13] J.L. Sussman, M. Harel, F. Frolow, et al., Atomic structure of acetylcholinesterase from Torpedo californica: a prototypic acetylcholine-binding protein, Science 253 (1991) 872–879, https://doi.org/10.1126/science.1678899.
[14] N.C. Inestrosa, A. Alvarez, C.A. Perez, et al., Acetylcholinesterase accelerates assembly of amyloid-β-peptides into Alzheimer's fibrils: possible role of the peripheral site of the enzyme, Neuron 16 (1996) 881–891, https://doi.org/10.1016/S0896-6273(00)80108-7.
[15] A.E. Reyes, M.A. Chacón, M.C. Dinamarca, et al., Acetylcholinesterase-Aβ complexes are more toxic than Aβ fibrils in rat hippocampus: effect on rat β-amyloid aggregation, laminin expression, reactive astrocytosis, and neuronal cell loss, Am. J. Pathol. 164 (2004) 2163–2174, https://doi.org/10.1016/S0002-9440(10)63774-1.
[16] C.S. Atwood, R.C. Scarpa, X. Huang, et al., Characterization of copper interactions with alzheimer amyloid β peptides: identification of an attomolar-affinity copper binding site on amyloid β1-42, J. Neurochem. 75 (2000) 1219–1233, https://doi.org/10.1046/j.1471-4159.2000.0751219.x.
[17] C. Opazo, X. Huang, R.A. Cherny, et al., Metalloenzyme-like activity of Alzheimer's disease β-amyloid Cu-dependent catalytic conversion of dopamine, cholesterol, and biological reducing agents to neurotoxic H2O2, J. Biol. Chem. 277 (2002) 40302–40308, https://doi.org/10.1074/jbc.M206428200.
[18] A.I. Bush, R.E. Tanzi, Therapeutics for Alzheimer's disease based on the metal hypothesis, Neurotherapeutics 5 (2008) 421–432, https://doi.org/10.1016/j.nurt.2008.05.001.
[19] Z. Najafi, M. Saeedi, M. Mahdavi, et al., Design and synthesis of novel anti-Alzheimer's agents: Acridine-chromenone and quinoline-chromenone hybrids, Bioorg. chem. 67 (2016) 84–94, https://doi.org/10.1016/j.bioorg.2016.06.001.
[20] A. Castro, A. Martinez, Peripheral and dual binding site acetylcholinesterase inhibitors: implications in treatment of Alzheimer's disease, Mini Rev. Med. Chem. 1 (2001) 267–272, https://doi.org/10.2174/1389557013406864.
[21] E.K. Perry, R. Perry, G. Blessed, et al., Changes in brain cholinesterases in senile dementia of Alzheimer type, Neuropathol. Appl. Neurobiol. 4 (1978) 273–277, https://doi.org/10.1111/j.1365-2990.1978.tb00545.x.
[22] N.H. Greig, T. Utsuki, D.K. Ingram, et al., Selective butyrylcholinesterase inhibition elevates brain acetylcholine, augments learning and lowers Alzheimer β-amyloid peptide in rodent, Proc. Natl. Acad. Sci. U.S.A. 102 (2005) 17213–17218, https://doi.org/10.1073/pnas.0508575102.
[23] F. Zemek, L. Drtinova, E. Nepovimova, et al., Outcomes of Alzheimer's disease therapy with acetylcholinesterase inhibitors and memantine, Expert Opin. Drug Saf. 13 (2014) 759–774, https://doi.org/10.1517/14740338.2014.914168.
[24] D.O. Ozgun, H.I. Gul, C. Yamali, et al., Synthesis and bioactivities of pyrazoline benzensulfonamides as carbonic anhydrase and acetylcholinesterase inhibitors with low cytotoxicity, Bioorg. chem. 84 (2019) 511–517, https://doi.org/10.1016/j.bioorg.2018.12.028.
[25] A. Biçer, P. Taslimi, G. Yakalı, et al., Synthesis, characterization, crystal structure of novel bis-thiomethylcyclohexanone derivatives and their inhibitory properties against some metabolic enzymes, Bioorg. chem. 82 (2019) 393–404, https://doi.org/10.1016/j.bioorg.2018.11.001.
[26] L. Ismaili, B. Refouvelet, M. Benchekroun, et al., Multitarget compounds bearing tacrine-and donepezil-like structural and functional motifs for the potential treatment of Alzheimer's disease, Prog. Neurobiol. 151 (2017) 4–34, https://doi.org/10.1016/j.pneurobio.2015.12.003.
[27] B. Sameem, M. Saeedi, M. Mahdavi, et al., A review on tacrine-based scaffolds as multi-target drugs (MTDLs) for Alzheimer's disease, Eur. J. Med. Chem. 128 (2017) 332–345, https://doi.org/10.1016/j.ejmech.2016.10.060.
[28] M. Singh, M. Kaur, N. Chadha, et al., Hybrids: a new paradigm to treat Alzheimer's disease, Mol. Divers. 20 (2016) 271–297, https://doi.org/10.1007/s11030-015-9628-9.
[29] K. Spilovska, J. Korabecny, E. Nepovimova, et al., Multitarget tacrine hybrids with neuroprotective properties to confront Alzheimer's disease, Curr. top. in med. chem. 17 (2017) 1006–1026, https://doi.org/10.2174/1568026605666160927152728.
[30] S.-Y. Li, N. Jiang, S.-S. Xie, et al., Design, synthesis and evaluation of novel tacrine–rhein hybrids as multifunctional agents for the treatment of Alzheimer's disease, Org. Biomol. Chem. 12 (2014) 801–814, https://doi.org/10.1039/c3ob42010h.
[31] S.-S. Xie, X. Wang, N. Jiang, et al., Multi-target tacrine-coumarin hybrids: cholinesterase and monoamine oxidase B inhibition properties against Alzheimer's disease, Eur. J. Med. Chem. 95 (2015) 153–165, https://doi.org/10.1016/j.ejmech.2015.03.040.
[32] D. Alonso, I. Dorronsoro, L. Rubio, et al., Donepezil–tacrine hybrid related derivatives as new dual binding site inhibitors of AChE, Bioorg. Med. Chem. 13 (2005) 6588–6597, https://doi.org/10.1016/j.bmc.2005.09.029.
[33] M.I. Rodríguez-Franco, M.I. Fernández-Bachiller, C. Pérez, et al., Novel tacrine−melatonin hybrids as dual-acting drugs for Alzheimer disease, with improved acetylcholinesterase inhibitory and antioxidant properties, J. Med. Chem. 49 (2006) 459–462, https://doi.org/10.1021/jm050746d.
[34] B. Bhrigu, D. Pathak, N. Siddiqui, et al., Search for biological active isatins: a short review, Int. J. Pharm. Sci. Drug Res. 2 (2010) 229–235.
[35] V. Raj, Review on CNS activity of isatin derivatives, Int. J. Curr. Pharm. Res 4 (2012) 1–9.
[36] J.F. Da Silva, S.J. Garden, A.C. Pinto, The chemistry of isatins: a review from 1975 to 1999, J. Braz. Chem. Soc. 12 (2001) (1975) 273–324, https://doi.org/10.1590/S0103-50532001000300002.
[37] S.N. Pandeya, S. Smitha, M. Jyoti, et al., Biological activities of isatin and its derivatives, Acta. Pharm. 55 (2005) 27–46.
[38] D.O. Ozgun, C. Yamali, H.I. Gul, et al., Inhibitory effects of isatin Mannich bases on carbonic anhydrases, acetylcholinesterase, and butyrylcholinesterase, J. Enzyme Inhib. Med. Chem. 31 (2016) 1498–1501, https://doi.org/10.3109/14756366.2016.1149479.
[39] N. Hamaue, M. Minami, M. Hirafuji, et al., Isatin, an endogenous MAO inhibitor, as a new biological modulator, CNS Drug Rev. 5 (1999) 331–346, https://doi.org/10.

1111/j.1527-3458.1999.tb00109.x.
[40] P. Riederer, W. Danielczyk, E. Grünblatt, Monoamine oxidase-B inhibition in Alzheimer's disease, Neurotoxicology 25 (2004) 271–277, https://doi.org/10.1016/S0161-813X(03)00106-2.
[41] L. Huang, C. Lu, Y. Sun, et al., Multitarget-directed benzylideneindanone derivatives: anti-β-amyloid (Aβ) aggregation, antioxidant, metal chelation, and monoamine oxidase B (MAO-B) inhibition properties against Alzheimer's disease, J. med. chem. 55 (2012) 8483–8492, https://doi.org/10.1021/jm300978h.
[42] A. Medvedev, O. Buneeva, O. Gnedenko, et al., Isatin interaction with glyceraldehyde-3-phosphate dehydrogenase, a putative target of neuroprotective drugs: partial agonism with deprenyl, in: Oxidative Stress and Neuroprotection, 2006, Springer, pp. 97–103. https://doi.org.10.1007/978-3-211-33328-0_11.
[43] A. Medvedev, O. Buneeva, O. Gnedenko, et al., Isatin, an endogenous nonpeptide biofactor: a review of its molecular targets, mechanisms of actions, and their biomedical implications, Biofactors 44 (2018) 95–108, https://doi.org/10.1002/biof.1408.
[44] P. Ershov, Y. Mezentsev, E. Yablokov, et al., Effect of Bioregulator Isatin on Protein-Protein Interactions Involving Isatin-Binding Proteins, Russ. J. Bioorgan. Chem. 44 (2018) 193–198, https://doi.org/10.1134/S1068162018010053.
[45] A. Medvedev, O. Buneeva, A. Kopylov, et al., The effects of endogenous non-peptide molecule isatin and hydrogen peroxide on proteomic profiling of rat brain amyloid-β binding proteins: relevance to Alzheimer's disease? Int. J. Mol. Sci. 16 (2015) 476–495, https://doi.org/10.3390/ijms16010476.
[46] K. Rakesh, H. Manukumar, D.C. Gowda, Schiff's bases of quinazolinone derivatives: synthesis and SAR studies of a novel series of potential anti-inflammatory and antioxidants, Bioorg. Med. Chem. Lett. 25 (2015) 1072–1077, https://doi.org/10.1016/j.bmcl.2015.01.010.
[47] A. Andreani, S. Burnelli, M. Granaiola, et al., New isatin derivatives with antioxidant activity, Eur. J. Med. Chem. 45 (2010) 1374–1378, https://doi.org/10.1016/j.ejmech.2009.12.035.
[48] M.M. Ismail, M.M. Kamel, L.W. Mohamed, et al., Synthesis of new indole derivatives structurally related to donepezil and their biological evaluation as acetylcholinesterase inhibitors, Molecules 17 (2012) 4811–4823, https://doi.org/10.3390/molecules17054811.
[49] Z. Omran, T. Cailly, E. Lescot, et al., Synthesis and biological evaluation as AChE inhibitors of new indanones and thiaindanones related to donepezil, Eur. J. Med. Chem. 40 (2005) 1222–1245, https://doi.org/10.1016/j.ejmech.2005.07.009.
[50] P.L. Gaikwad, P.S. Gandhi, D.M. Jagdale, et al., The use of bioisosterism in drug design and molecular modification, Am. J. PharmTech Res. 2 (2012) 1–23.
[51] P. Costanzo, L. Cariati, D. Desiderio, et al., Design, synthesis, and evaluation of donepezil-like compounds as AChE and BACE-1 inhibitors, ACS Med. Chem. Lett. 7 (2016) 470–475, https://doi.org/10.1021/acsmedchemlett.5b00483.
[52] A. Rampa, F. Mancini, A. De Simone, et al., From AChE to BACE1 inhibitors: the role of the amine on the indanone scaffold, Bioorg. Med. Chem. Lett. 25 (2015) 2804–2808, https://doi.org/10.1016/j.bmcl.2015.05.002.
[53] J.S.D. Costa, D.S. Pisoni, C.B.D. Silva, et al., Lewis acid promoted Friedländer condensation reactions between anthranilonitrile and ketones for the synthesis of tacrine and its analogues, J. Braz. Chem. Soc. 20 (2009) 1448–1454, https://doi.org/10.1590/S0103-50532009000800009.
[54] M.S. Alam, J.-H. Choi, D.-U. Lee, Synthesis of novel Schiff base analogues of 4-amino-1, 5-dimethyl-2-phenylpyrazol-3-one and their evaluation for antioxidant and anti-inflammatory activity, Bioorg. Med. Chem. 20 (2012) 4103–4108, https://doi.org/10.1016/j.bmc.2012.04.058.
[55] G.L. Ellman, K.D. Courtney, V. Andres Jret al., A new and rapid colorimetric determination of acetylcholinesterase activity, Biochem. Pharmacol. 7 (1961) 88–95, https://doi.org/10.1016/0006-2952(61)90145-9.
[56] T.C. Dinis, V.M. Madeira, L.M. Almeida, Action of phenolic derivatives (acetaminophen, salicylate, and 5-aminosalicylate) as inhibitors of membrane lipid peroxidation and as peroxyl radical scavengers, Arch. Biochem. Biophys. 315 (1994) 161–169 https://www.ncbi.nlm.nih.gov/pubmed/7979394.
[57] V. Aparadh, V. Naik, B. Karadge, Antioxidative properties (TPC, DPPH, FRAP, metal chelating ability, reducing power and TAC) within some Cleome species, Annali di Botanica 2 (2012) 49–56, https://doi.org/10.4462/annbotrm-9958.
[58] N. Salehi, B.B.F. Mirjalili, H. Nadri, et al., Synthesis and biological evaluation of new N-benzylpyridinium-based benzoheterocycles as potential anti-Alzheimer's agents, Bioorg. chem. 83 (2019) 559–568, https://doi.org/10.1016/j.bioorg.2018.11.010.
[59] R. Sudan, M. Bhagat, S. Gupta, et al., Iron (FeII) chelation, ferric reducing antioxidant power, and immune modulating potential of Arisaema jacquemontii (Himalayan Cobra Lily), Biomed Res. Int. 2014 (2014), https://doi.org/10.1155/2014/179865.
[60] H. Levine III, Thioflavine T interaction with synthetic Alzheimer's disease β-amyloid peptides: Detection of amyloid aggregation in solution, Protein Sci. 2 (1993) 404–410, https://doi.org/10.1002/pro.5560020312.